

Modeling metal-sediment interaction processes: Parameter sensitivity assessment and uncertainty analysis



Eunju Cho^a, George B. Arhonditsis^b, Jeehyeong Khim^{a,*}, Sewoong Chung^{c,**},
Tae-Young Heo^d

^a School of Civil, Environmental and Architectural Engineering, Korea University, Seoul, 136-701, South Korea

^b Ecological Modeling Laboratory, Department of Physical & Environmental Sciences, University of Toronto, Toronto, Ontario, M1C 1A4, Canada

^c Department of Environmental Engineering, Chungbuk National University, Cheongju, 362-763, South Korea

^d Department of Information & Statistics, Chungbuk National University, Cheongju, 362-763, South Korea

ARTICLE INFO

Article history:

Received 7 July 2015

Received in revised form

20 November 2015

Accepted 22 February 2016

Available online xxx

Keywords:

Sediment-metal modeling

Parameter uncertainty analysis

Sensitivity analysis

Bayesian Monte Carlo

EFDC

Geum river

ABSTRACT

Sensitivity and uncertainty analysis of contaminant fate and transport modeling have received considerable attention in the literature. In this study, our objective is to elucidate the uncertainty pertaining to micropollutant modeling in the sediment-water column interface. Our sensitivity analysis suggests that not only partitioning coefficients of metals but also critical stress values for cohesive sediment affect greatly the predictions of suspended sediment and metal concentrations. Bayesian Monte Carlo is used to quantify the propagation of parameter uncertainty through the model and obtain the posterior parameter probabilities. The delineation of periods related to different river flow regimes allowed optimizing the characterization of cohesive sediment parameters and effectively reducing the overall model uncertainty. We conclude by offering prescriptive guidelines about how Bayesian inference techniques can be integrated with contaminant modeling and improve the methodological foundation of uncertainty analysis.

© 2016 Elsevier Ltd. All rights reserved.

1. Introduction

Micropollutants often represent a major threat to the integrity of surface waters, such as rivers, lakes, and estuaries (Hong et al., 2003; Moldovan, 2006). The complex interplay between physical and biogeochemical processes that modulates micropollutant concentrations has received considerable attention in the recent literature. Mathematical modeling offers a comprehensive means to simulate fate and transport of heavy metals/organic contaminants and to support water quality management decisions that effectively protect aquatic ecosystem functioning (Ongley et al., 1992; Ji et al., 2002; Chu and Rediske, 2012). For example, mathematical models are an integral component of all the total maximum

daily load (TMDL) programs in order to determine optimal management actions that can control point and non-point pollution sources and ultimately achieve water quality standards (National Research Council, 2001).

The typical practices in micropollutant modeling view model calibration as an inverse solution problem, whereby model parameters are iteratively adjusted until the discrepancy between model outputs and observed data is minimized (Freni and Mannina, 2010). This procedure may potentially offer insights into the magnitude of ecosystem processes/causal mechanisms that shape micropollutant concentrations, but it is frequently undermined by the well-known equifinality (poor model identifiability) problem, where several distinct choices of model inputs lead to the same model outputs (many sets of parameters fit the data about equally well) (Arhonditsis et al., 2007). A main reason for the equifinality problem is that the processes used for understanding how the system works internally is of substantially higher order than what can be externally observed. Moreover, while these modeling constructs can be complex and contain significant mechanistic foundation, their application involves uncertainty contributed by model structure and parameters as well as measurement imprecision and

* Corresponding author. School of Civil, Environmental and Architectural Engineering, Korea University, Anam-dong, Seongbuk-gu, Seoul, 136-701, South Korea.

** Corresponding author. Department of Environmental Engineering, Chungbuk National University, Chungdae-ro 1, Seowon-gu, Cheongju, Chungbuk, 362-763, South Korea.

E-mail addresses: hyeong@korea.ac.kr (J. Khim), schung@chungbuk.ac.kr (S. Chung).

other data uncertainties. The structural uncertainty is not surprising because all models are drastic simplifications of reality that approximate the actual processes, i.e., essentially, all parameters are effective (spatially and temporally averaged) values unlikely to be represented by a fixed constant (Arhonditsis et al., 2007, 2008a,b). Furthermore, heavy metal/organic contaminant data are expensive, scarce, and highly variable (Freni and Mannina, 2010; Vezzaro and Mikkelsen, 2012), so individual equations which are approximately correct in controlled laboratory environments may not collectively yield an accurate picture of the processes that shape micropollutant concentrations in surface waters (Reichert, 1997; Refsgaard et al., 2005; Krysanova et al., 2007). Therefore, uncertainty analysis has been a topic of increasing importance in hydrological and water quality modeling (Freni et al., 2009; Torres and Bertrand-Krajewski, 2008; Marsili-Libelli and Giusti, 2008; Arhonditsis, 2008a,b; Shen et al., 2012; Ruark et al., 2011). Although several techniques have been implemented to evaluate parametric uncertainty (Sohn et al., 2000; Freni and Mannina, 2010), the effects of model parameters on predicted results are not well understood and can vary depending on the characteristics of modeled contaminants (Sommerfreund et al., 2010; Matthies et al., 2004).

One of the most challenging processes in micropollutant modeling is the reproduction of their adsorption on the surface of cohesive sediments and their subsequent transport in the water column (Ji, 2008; Trento and Alvarez, 2011; Liu et al., 2012). In this regard, Liu et al. (2012) simulated the two-dimensional transport and distribution of heavy metals along the tidal Keelung River estuary, indicating that the partition coefficient plays an important role in the distribution of dissolved and particulate lead concentrations. In the same context, Trento and Alvarez (2011) evaluated the relative parameter sensitivity of a simple model that aimed to simulate chromium and fine sediment transport, showing that the characterization of the associated processes was predominantly driven by several parameters, such as the partition coefficients in the water column and bed sediments, the depth of the active bed sediment layer, and the mass transfer coefficient between the water column and sediment pore water. Along the same line of reasoning, Franceschini and Tsai (2010) underscored the importance of the characterization of suspended sediment processes, when modeling total polychlorinated biphenyls (PCBs) with Environmental Fluid Dynamics Code (EFDC) and Water Quality Analysis Simulation Program (WASP). Many other studies similarly emphasized that the modules that simulate toxic micropollutant concentrations are particularly sensitive to parameters related to cohesive sediments, such as settling velocity, critical stress values on sediment bed as well as to the metal partitioning coefficients (Shen et al., 2010,

2012; Ruark et al., 2011). To make matters worse, the spatial and temporal heterogeneity of the associated physical and chemical processes are important confounding factors that can profoundly inflate model uncertainty (Sohn et al., 2000; Kanso et al., 2005; Franceschini and Tsai, 2010).

In this study, our first objective is to shed light on how the uncertainty of the outputs of micropollutant modeling can be apportioned to five critical parameters; namely, the settling velocity (w_s), critical deposition stress (τ_{cd}), critical erosion stress (τ_{ce}), metal partitioning coefficient between suspended sediment and water column ($K_{d,ss}$), and metal partitioning coefficient between sediment bed and water column ($K_{d,bed}$). Specifically, we evaluate the efficiency of the local or one-step-at-a-time (OAT) sensitivity analysis method relative to the Morris Screening method. In a subsequent exercise, we implement the Bayesian Monte Carlo method to quantify uncertainty propagation of model parameters and derive posterior parameter probabilities based on the corresponding priors and observed data. Our study concludes by offering prescriptive guidelines about how Bayesian inference techniques can be integrated with contaminant modeling in order to improve the methodological foundation of uncertainty analysis.

2. Methods

2.1. Model setup-data sources

The study site for this investigation is located in the middle reach of Geum River, one of the four major rivers in Korea, where two multipurpose dams have been built. The spatial model domain begins from the Daechong Regulation Dam to Maeogu, with a total length of 36,740 m. The cell map was constructed using a SMS (surface-water modeling system) program based on the data modification obtained from the Korean Ministry of Land, Infrastructure, and Transport (Fig. 1). There were a total of 273 active cells, which were formed by 83 longitudinal and 8 lateral cells. The average cell length and width were 429.8 m and 151.7 m, respectively. Because the construction period of the Sejongbo Dam, which included movable and fixed weirs, was from May 2009 to June 2012, different elevation data were used in 2011 and 2012 to incorporate the changes of bottom topography over time.

In this paper, we implemented the Environmental Fluid Dynamics Code (EFDC) Explorer 7, a widely used model with the capability to simulate the cohesive sediment transport and metal behavior (Elçi et al., 2007; Ji et al., 2002), developed by Dynamic Solutions International (DSI). Model calibration and verification was based on water surface elevation data measured at Hyundo

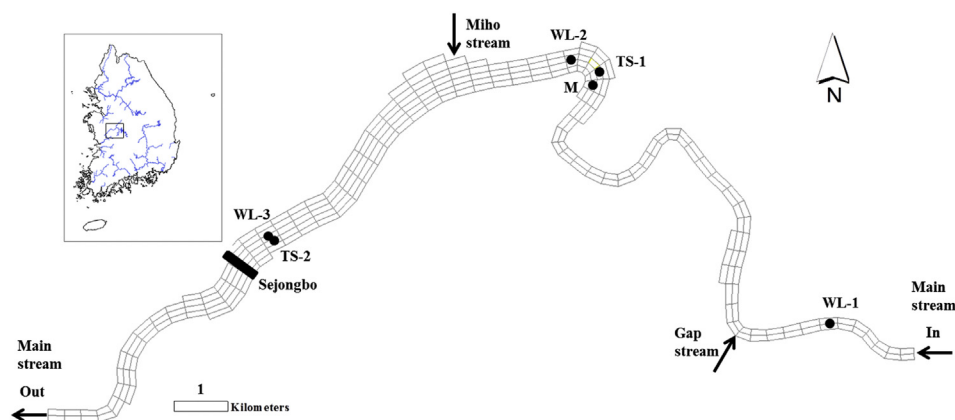


Fig. 1. Location of the Geum River in Korea, and the cell map with the boundaries and monitoring points of the water surface elevation (WL-1, WL-2, WL-3), temperature and total suspended sediment concentrations (TS-1, TS-2), and total and dissolved metal concentrations (M).

(WL-1), Bugang (WL-2), and Geumnam (WL-3) stations, water temperature and sediment concentrations from Geumbon-G (TS-1) and Geumbon-H (TS-2) stations, and heavy metal concentrations from Chungwon (M) station. Flow boundary conditions, including the inflow from the main stream, Gap stream, and Miho stream and the flow through the Sejongbo dam, were obtained from K-water's hydrological database, as shown in Fig. S1 (K-Water, 2014). Meteorological data were obtained from the Daejeon weather station (Fig. S2). The total and dissolved metal concentrations in the water and data related to the sediment bed characteristics were compiled from reports by the Korean Ministry of Environment (KME) (KME, 2011a, 2012a; KME, 2011b, 2012b). Details are shown in the Supporting Information section (Tables S1–S2 & Figs. S1–S3). The focal metal for our modeling study is cadmium (Cd). The total metal concentration is the sum of the particulate concentration adsorbed on the suspended cohesive sediment and the dissolved concentration in water. The effect of pH was not considered because pH variability in the study site was minimal $7.49\text{--}7.73 \pm 0.25\text{--}0.41$ (KME, 2014). The variation of the partitioning coefficient for cadmium due to pH variability is also negligible (Sauve et al., 2000). The model was run for two 6-month monitoring periods from July 1 through December 31 in 2011 and 2012, respectively. The former data set (2011) was used for calibration, while the latter set (2012) was used for validation (or predictive confirmation). A 5-sec time step was used for all simulations. For simplicity, the hydrodynamic equations, the sediment behavior and numerical schemes of the EFDC model will not be presented in this paper, but are detailed in Hayter and Mehta (1983), Hamrick (1992), Hamrick and Wu (1997), and Ji et al. (2002).

2.2. Sensitivity analysis

As previously mentioned, we applied two sensitivity analysis strategies; the local or one-step-at-a-time (OAT) and the Morris Screening or elementary effects method. Our focus was on the impact of five input parameters on the predictions of cohesive sediment concentrations, total and dissolved metal concentrations in water: settling velocity (w_s), critical deposition stress (τ_{cd}), critical erosion stress (τ_{ce}), metal partitioning coefficient between suspended sediment and water column ($K_{d,SS}$), and metal partitioning coefficient between sediment bed and water column ($K_{d,bed}$).

The OAT method is the most frequently applied technique in the modeling literature (Saltelli and Annoni, 2010; Sun et al., 2012). Output variations are evaluated with respect to fractional change of one input parameter, while the other parameters are held constant. In this study, each input parameter was perturbed by $\pm 50\%$ relative to its reference value (see also reasoning for the range selection provided in Table S3). The reference parameter values were based on the calibration vector (see Section 3.1). The sensitivity of the i th input parameter is calculated by:

$$\text{Sensitivity} = \frac{\theta_i \times E\left[\left|y_j - y_0\right|\right]}{\delta\theta_i \times E[y_0]} \times 100(\%)$$

where θ_i is the perturbed input parameter, y_j is the output variable after the parameter perturbation, y_0 is the output obtained by the reference (calibration) parameter value, and $\delta\theta_i$ is the variation of the i th parameter. The outputs y_j and y_0 were obtained over the entire spatial (273 cells) and temporal (July 2011 to December 2012 or 368 days) domain of our analysis; that is, the variation of the output ($y_j - y_0$) was calculated for each cell and point in time. In particular, the absolute discrepancies were calculated to prevent the results from canceling each other out, and thus obtain the

averaged value of total variation $E[|y_i - y_0|]$, due to changes of the i th input parameter over the entire simulated space and time (Freni and Mannina, 2010).

Using the local method though, it is not always possible to distinguish which parameters are more influential, because the individual effects of a particular parameter are also conditional upon the parameter values assigned to the rest elements of the input vector (Sun et al., 2012). Even if the parameters are independent of each other, the results may still be different due to non-linearities in model behavior, which cannot necessarily be captured by single-parameter perturbations (Campolongo and Saltelli, 2000; Saltelli et al., 2007; Norton, 2009). To overcome the technical weaknesses of the local method, we considered the Morris screening (or elementary effects) method, as an appealing alternative in which the input vector is scrutinized to obtain the ranking of input parameters in terms of their importance, while accommodating any issues of non-linearity and/or interactions with other parameters (Morris, 1991; Saltelli et al., 2002; Neumann, 2012). The Morris screening method is briefly described below and is detailed elsewhere (Morris, 1991). Derived from basic statistics, this method computes the elementary effect d_i by calculating the model output variations induced by a number of incremental changes of each input parameter θ_i ($i = 1, \dots, k$). This is expressed as:

$$d_i(\theta_i) = \frac{|y(\theta_1, \dots, \theta_{i-1}, \theta_i + \Delta, \theta_{i+1}, \dots, \theta_k) - y(\theta_1, \dots, \theta_{i-1}, \theta_i, \theta_{i+1}, \dots, \theta_k)|}{\Delta}$$

where the vector $(\theta_1, \dots, \theta_{i-1}, \theta_i, \theta_{i+1}, \dots, \theta_k)$ is randomly sampled within the quantile space of the parameters, Δ is the perturbation, and p is the number of levels. The input parameter space is assumed to be uniformly distributed and converted to a unit hypercube. Each of the k input parameters is divided into p levels; thus, the parameter space sampled is configured as a k -dimensional, p -level grid. The ranges assigned to the five input parameters are explained in the next paragraph. Because the elementary effect d_i depends on the location of the random sample, the calculations at different locations are repeatedly performed r times. According to Campolongo et al. (2007), the repetition value r is typically chosen between 10 and 50. The average elementary effect μ_i and standard deviation σ_i computed from the cumulative distribution $F(d_i)$ of the r elementary effects indicates the overall influence of the input factor on the output and the combination of the factor's higher order effects (i.e., non-linear and/or interaction effects), respectively. These two measures need to be read together in order to rank the relative importance of parameter inputs and identify those parameters which do (or do not) influence the output variability. Low values of both μ_i and σ_i correspond to a non-influential parameter. In this study, because the negative and positive values of d_i might cancel each other out when calculating the average elementary effect μ_i , the mean of the absolute value of the elementary effects μ_i^* was used as an indicator of the parameter sensitivity, which Campolongo et al. (2007) proposed to accommodate any non-monotonic patterns in model behavior. This method has been successfully applied in water quality modeling (Sun et al., 2012; Neumann, 2012; Gamerith et al., 2013). The required number of simulations to compute r replicates of the elementary effects for k parameters is $N = r \times (k+1)$ (Morris, 1991). The present case study is based on the typical specification in which $p = 4$, $\Delta = p/(2 \times (p-1)) = 2/3$, and $r = 10$, thereby requiring a total of $N = 10 \times (5 + 1) = 60$ simulations. The outputs were obtained from the 273 total cells and the entire 368 days; thus, the elementary effect and standard deviation were averaged over the total number of cells and simulation time.

Experimental data for the five input parameters were not available, and thus literature review was used to compile the

parameter values (Table 1). The presence of the Sejongbo Dam rendered both river and lake characteristics in our case study and therefore our review aimed to capture a broad range of cohesive sediments. Hwang et al. (2006, 2008), Ryu et al. (2006), and Gunsan Regional Oceans and Fisheries Administration (2010) reported settling velocity and critical erosion stress values from Geum estuary that ranged from 9.0×10^{-6} to 10^{-3} m/sec and from 0.12 to 0.41 N/m², respectively. The corresponding values from the international literature vary considerably, ranging from 1.5×10^{-4} to 2.0×10^{-3} m/sec and 0.115–0.93 N/m² for settling velocity and critical erosion stress, respectively (Villaret and Paulic, 1986; Ji et al., 2002; Kim, 2002; Trento and Alvarez, 2011; Liu et al., 2012; Chu and Rediske, 2012; Wang et al., 2013). In the case of critical deposition stress, there were no data available from Geum estuary and the values used were obtained from the EFDC manual and other literature sources, ranging from 0.02 to 1.1 N/m² (Mehta, 1986; Onishi et al., 1993; Ji et al., 2002; Kim, 2002; Tetra Tech, Inc., 2007; Liu et al., 2012; Wang et al., 2013). In the case of metal partitioning coefficients, the parameter ranges assigned were lying within the ± 1.96 standard deviation (approximately 95% confidence intervals) of the empirical distributions of the EPA report (Allison and Allison, 2005).

2.3. Uncertainty analysis

The Bayesian Monte Carlo method quantifies model parameter uncertainty by updating the probabilities of model parameters (posteriors) as a function of the corresponding prior distributions and observed data. Simply put, the posterior probability of a specific parameter is derived as the joint effect of any knowledge regarding the relative plausibility of its values prior to the data collection and the likelihood of model predictions given the dataset at hand. This is expressed as follows:

$$P(\theta|D) = \frac{P(D|\theta)P(\theta)}{\int P(D|\theta)P(\theta)d\theta}$$

where θ is the uncertain model parameter, D is the observation, $P(\theta|D)$ is the posterior probability, $P(D|\theta)$ is the likelihood function, and $P(\theta)$ is the prior probability. The likelihood function is formulated with an error model, which assumes that the residuals between the observations D and the model predictions Y are normally

distributed with a zero mean and constant variance σ^2 .

$$P(D|\theta) = \frac{1}{\sqrt{2\pi\sigma^2}} \exp\left[-\frac{(D-Y)^2}{2\sigma^2}\right]$$

Monte Carlo analysis was used to sample the prior probabilities of the model parameters. For the purpose of the present uncertainty analysis, we generated Monte Carlo sample sizes of 20, 100, 500, 1000, and 5000. Each model parameter was assumed to be uniformly distributed within the ranges assigned during our sensitivity analysis (Table 1). To effectively sample the prior parameter space, we used Latin Hypercube Sampling. The standard deviation of the residuals (σ) between observations and corresponding model predictions was evaluated for each iteration, assuming homoscedasticity of the residuals (Camacho and Martin, 2013). The likelihood function considers all the independent observations for a particular modeled variable. For example, with 91 measurements of total suspended sediment concentrations ($j = 1, \dots, 91$) from two monitoring points TS-1 and TS-2 in Fig. 1 ($i = 1, 2$), the corresponding likelihood function is:

$$P(D|\theta) = \prod_{i=1}^2 \prod_{j=1}^{91} \frac{1}{\sqrt{2\pi\sigma^2}} \exp\left[-\frac{(D_{ij} - Y_{ij})^2}{2\sigma^2}\right]$$

With this approach, the settling velocity, critical deposition stress, and critical erosion stress of the cohesive sediments were updated using the total suspended sediment concentrations. The total metal concentrations were similarly used to update the three parameters of the cohesive sediments and the suspended sediment-water partitioning coefficient. Finally, the dissolved metal concentrations were used to update the five model parameters. The uncertainty bands of the prior and posterior predictive distributions of the total suspended sediment concentration, total metal concentration, and dissolved metal concentration over each period were calculated, and the uncertainties of each concentration were estimated from their average and maximum values. Wider bands indicate higher uncertainty and lower confidence in the model outputs, whereas narrower bands indicate higher model reliability (Freni and Mannina, 2010). For illustration purposes, our uncertainty analysis was conducted for one model state variable at a time, although we note that our on-going research focuses on more complex uncertainty analysis frameworks that accommodate

Table 1
Range of values assigned to the model calibration parameters.

Input parameter	Unit	Range	Source
Settling velocity (w_s)	m/s	$9.0 \times 10^{-6} - 2.0 \times 10^{-3}$	a–f, g, n
Critical deposition stress (τ_{cd})	N/m ²	$2.0 \times 10^{-2} - 1.1 \times 10^0$	a, b, d, g, k, l, m
Critical erosion stress (τ_{ce})	N/m ²	$1.2 \times 10^{-1} - 9.3 \times 10^{-1}$	a, b, d, g–j
Cd partitioning coefficient between suspended sediment and water ($K_{d,ss}$)	L/mg	$5.0 \times 10^{-3} - 1.3 \times 10^0$	o
Cd partitioning coefficient between sediment bed and water ($K_{d,bed}$)	L/mg	$3.2 \times 10^{-6} - 4.2 \times 10^0$	o

^aWang et al. (2013).

^bJi et al. (2002).

^cChu and Rediske (2012).

^dLiu et al. (2012).

^eTrento and Alvarez (2011).

^fHwang et al. (2006).

^gKim (2002).

^hHwang et al. (2008).

ⁱRyu et al. (2006).

^jVillaret and Paulic (1986).

^kTetra Tech, Inc (2007).

^lMehta (1986).

^mOnishi et al. (1993).

ⁿGunsan Regional Oceans and Fisheries Administration (2010).

^oAllison and Allison (2005).

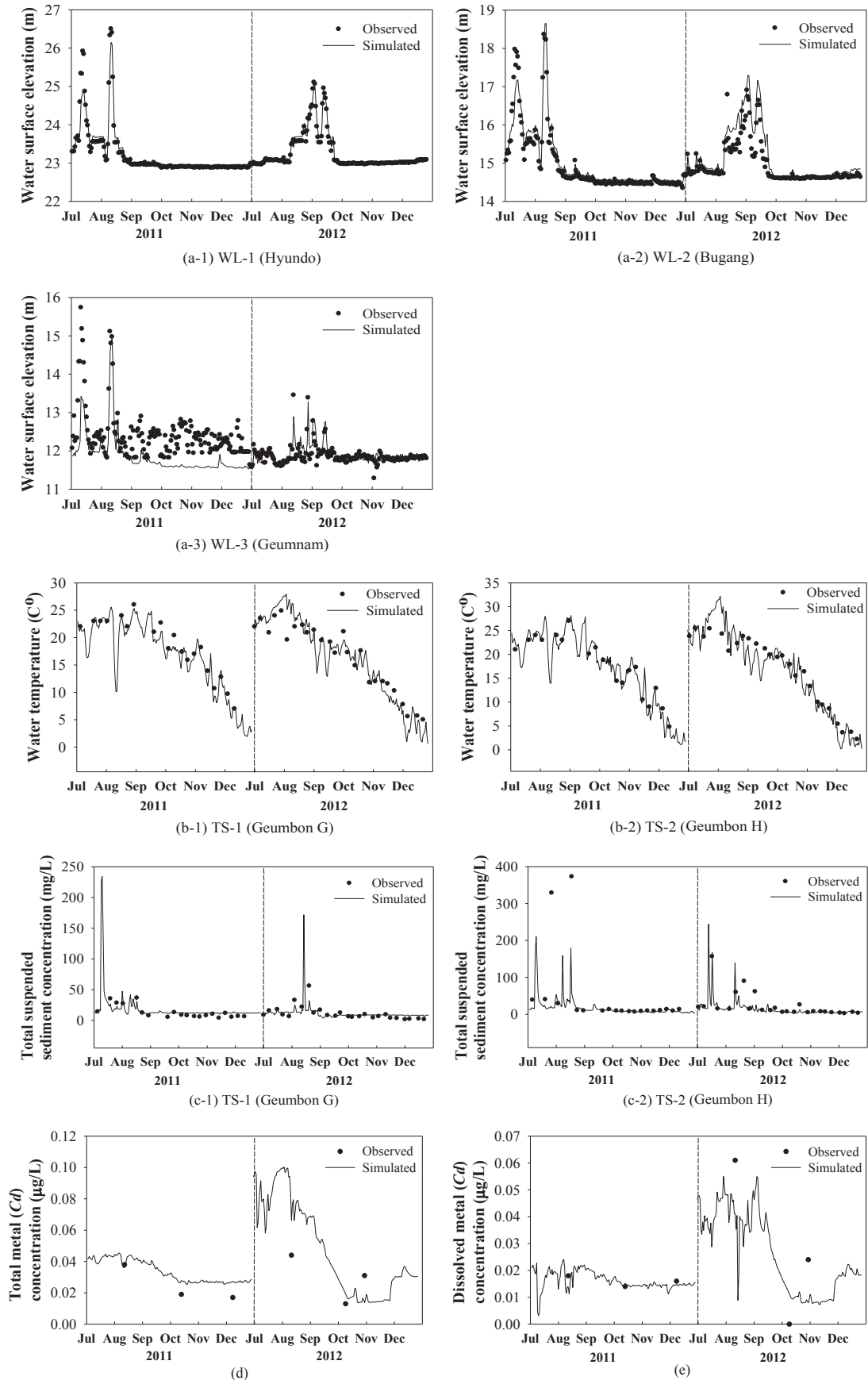


Fig. 2. Measured values and model outputs along Geum River from July to December in 2011 and 2012: (a-1)-(a-3) water surface elevation, (b-1)-(b-2) water temperature, (c-1)-(c-2) total suspended sediment concentration, (d) total metal (Cd) concentration, and (e) dissolved metal (Cd) concentration.

different assumptions about the dependence patterns among multiple model endpoints (Ramin and Arhonditsis, 2013).

3. Results-discussion

3.1. Model calibration-sensitivity analysis

Parameter values assigned during the model calibration were 2.2×10^{-4} m/sec for settling velocity, 0.2 N/m^2 for critical deposition stress, 0.4 N/m^2 for critical erosion stress, 0.079 L/mg for C_d partitioning coefficient between suspended sediment and water, and 0.002 L/mg for C_d partitioning coefficient between sediment bed and water. Time series comparisons between modeled and measured water elevation, temperature, total suspended sediment, total C_d , and dissolved C_d concentrations for the calibration and validation periods are presented in Fig. 2. Table 2 summarizes the error assessment based on Absolute Mean Error (AME), Root Mean Square Error (RMSE), Relative Error (RE), and Relative Root Mean Square Error (RRMSE) (Ji, 2008; see also error formulations in Table S4 in our Supporting Information section). We obtained satisfactory fit between simulated and measured values for water surface elevation, temperature, and total suspended sediment concentrations. It is also interesting to note that model performance was fairly similar between the calibration and validation domains. On the other hand, the model failed to capture several peaks of total suspended sediment concentrations that occurred during the high flow season (August–September) in Geumbon H (station in TS 2). This discrepancy likely stems from a misspecification of the boundary conditions, as the cohesive and non-cohesive suspended sediment concentrations were not separately monitored, and therefore our simulations were based on a fixed ratio obtained from local reports (KME, 2010; KME, 2011b, 2012b). Likewise, the model was characterized by significant discrepancy between observed and modeled C_d concentrations; especially in

the extrapolation (validation) domain. The simulated total and dissolved metal concentrations increased as a result of the high flow rates and sediment re-suspension during July–September (Fig. 2), but the RRMSEs ranged from 26% to 66% and were much higher than the error values obtained for water surface elevation, temperature, and total suspended sediment concentrations.

The relative influence of input parameters to model outputs was quantified for the entire simulation period and separately for the high (July to September) and low flow (October to December) seasons, as determined by the local rainfall patterns (Table 3; Fig. 3 & Fig. 4a). Critical erosion stress (τ_{ce}) was identified to be a particularly influential parameter to total suspended sediment, total and dissolved C_d concentrations (Fig. 3). The suspended sediment predictions are modulated by the vertical exchange mechanisms between water column and sediment bed. According to EFDC model, the net sediment flux ($J_0 = J_d - J_r$) is equal to the difference between total sediment deposition (J_d) and erosion (resuspension) fluxes (J_r) (Ziegler and Nisbet, 1994, 1995; Ji, 2008). The former flux is a function of the critical deposition stress and settling velocity, while the latter one is a function of the critical erosion stress. If the critical erosion stress is lower than the bed shear stress exerted by the flow, the sediment bed is eroded and the suspended sediment concentration in the water column subsequently increases. Parameters related to the characterization of bottom boundary conditions, i.e., the critical bed-shear stresses for erosion and particulate settling rate, are critical to the outputs of micropollutant modeling and this finding consistently emerges when conducting both first-order and global sensitivity analysis (Maa et al., 2008; Ruark et al., 2011). Interestingly, our analysis also showed that the perturbations induced to parameters related to the behavior of cohesive sediments had a greater impact to the total and dissolved metal concentrations than to the suspended sediment concentrations. Because of their high adsorptive affinity, heavy metals are attached to cohesive sediments and can be subject to transportation, deposition, and/or erosion (Ongley et al., 1992; Ji et al., 2002; Zaramella et al., 2006; Chu and Rediske, 2012). For strongly adsorptive heavy metals, suspended sediments often play a critical role in their fate and therefore sediment bed may function as a major sink or source (Liu et al., 2012; Trento and Alvarez, 2011; Ji, 2008; Yang et al., 2012); thus, the sensitivity of total and dissolved metal concentrations to changes of the corresponding parameters is not surprising.

We also found that the relative importance of model parameters is characterized by significant variability between the two flow-related seasons. A characteristic example is the derived sensitivities of cohesive sediment parameters, which were higher during the low relative to the high flow season (Fig. 3b–c & Table 3). East Asian monsoons bring heavy rainfall to South Korea during a short period of time between July and September, whereas the rest of the year (October to December) is relatively dry (Fig. 4a). As shown in Fig. 4b, the simulated bed shear stress was always greater than the calibrated value of the critical stresses, caused by increased flow due to heavy rain, and thus when the corresponding input parameters were changed, the variation in the suspended cohesive sediment, total/dissolved C_d concentrations was fairly minimal. By contrast, the simulated bed shear stress hovered around the critical stress values during low flow conditions and therefore the perturbations induced during the sensitivity analysis triggered regime shifts with respect to the nature of the sediment-water column interactions. Thus, the influence of the cohesive sediment parameters was generally higher in the dry (Period 2) relative to the wet season (Period 1). For the suspended sediment concentrations, the most sensitive parameter was the critical erosion stress, followed by settling velocity and critical deposition stress. The same sensitivity rankings were also derived for total C_d concentrations. By

Table 2

Model error analysis: (a) water surface elevation, (b) water temperature, (c) total suspended sediment concentration, (d) total metal concentration, and (e) dissolved metal concentration. The locations of each sampling point are shown in Fig. 1.

	(a-1) WL-1		(a-2) WL-2		(a-3) WL-3	
	2011	2012	2011	2012	2011	2012
AME (m)	0.0656	0.0400	0.1503	0.1935	0.5622	0.1130
RMSE (m)	0.1585	0.0601	0.2123	0.3009	0.6889	0.1622
RE (%)	0.2827	0.1723	1.0043	1.2958	4.5258	0.9524
RRMSE (%)	4.3734	2.7818	5.2835	12.9759	17.5785	7.4752
	(b-1) TS-1		(b-2) TS-2			
	2011	2012	2011	2012		
AME (°C)	1.0359	1.5654	1.0554	1.8353		
RMSE (°C)	1.3277	1.9426	1.4709	2.2505		
RE (%)	5.6344	9.4629	5.9981	10.8933		
RRMSE (%)	6.9881	9.7619	6.6256	9.6588		
	(c-1) TS-1		(c-2) TS-2			
	2011	2012	2011	2012		
AME (mg/L)	4.4505	4.5418	35.2332	8.7508		
RMSE (mg/L)	4.8987	6.2696	99.2797	17.9352		
RE (%)	34.2217	41.1735	73.3186	37.4608		
RRMSE (%)	15.0267	11.5039	27.1034	11.6236		
	(d)		(e)			
	2011	2012	2011	2012		
AME (µg/L)	0.0070	0.0153	0.0022	0.0157		
RMSE (µg/L)	0.0079	0.0167	0.0026	0.0161		
RE (%)	28.4465	52.0619	13.7799	55.4465		
RRMSE (%)	37.5769	53.7689	66.1123	26.3652		

Table 3

Averaged sensitivity values from the OAT method when the model input parameter was increased and decreased by 50% from its calibrated value. All reported values are percentages, and bold numbers indicate the most sensitive parameter in that period.

Input parameter	Cohesive sediment concentration			Total metal concentration			Dissolved metal concentration		
	Total	Period 1	Period 2	Total	Period 1	Period 2	Total	Period 1	Period 2
Settling velocity (w_s)	3.60	2.33	5.72	14.33	2.90	24.14	22.55	2.15	35.34
Critical deposition stress (τ_{cd})	2.96	1.69	5.07	21.96	1.74	39.32	38.82	1.36	62.29
Critical erosion stress (τ_{ce})	8.56	4.79	14.86	33.59	6.89	56.51	38.90	6.87	58.97
Cd partitioning coefficient between suspended sediment and water ($K_{d,SS}$)	–	–	–	–	–	–	34.85	50.50	25.04
Cd partitioning coefficient between sediment bed and water ($K_{d,bed}$)	–	–	–	1.74	0.71	2.63	1.92	0.95	2.52

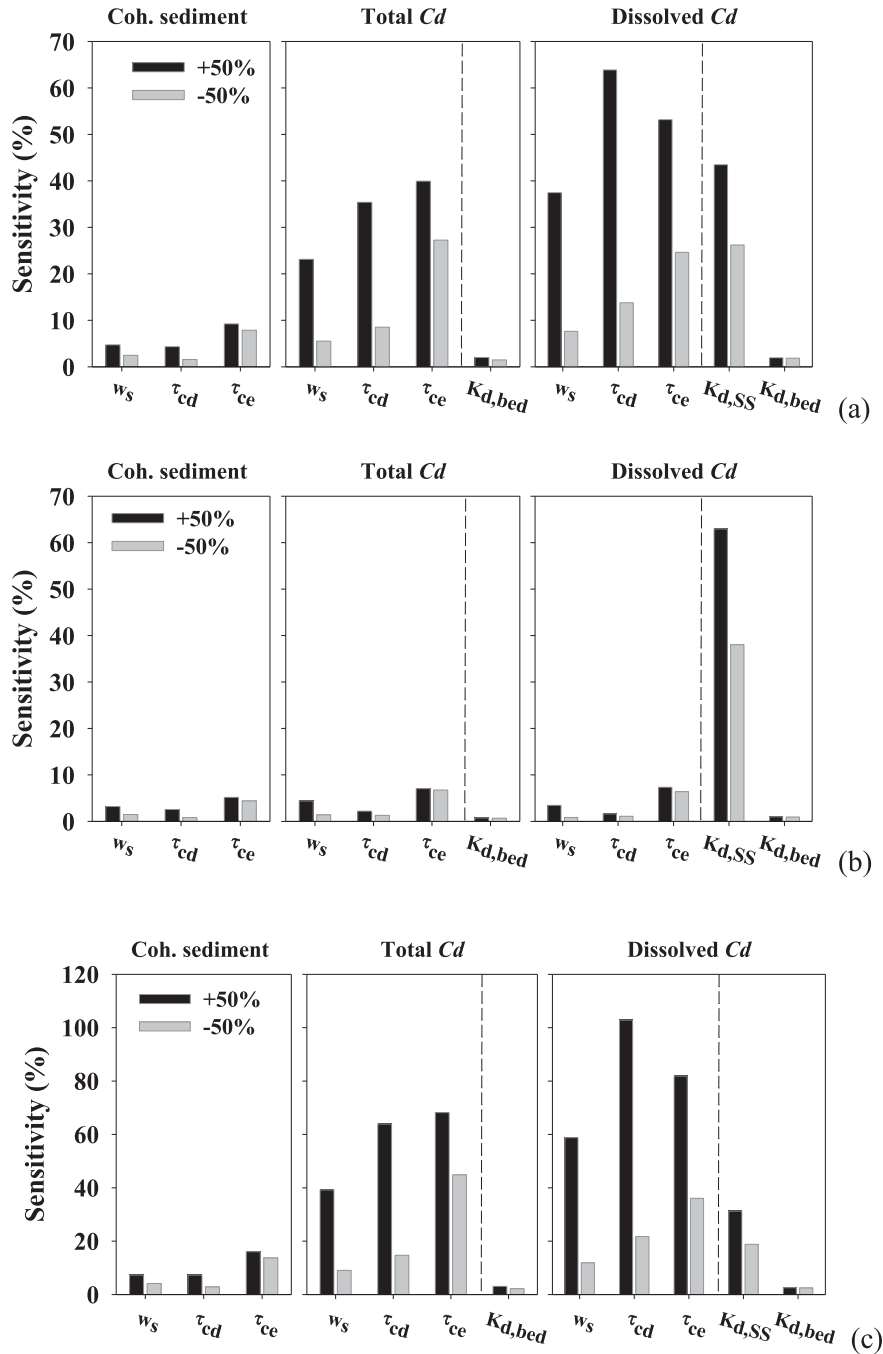


Fig. 3. Sensitivity values of the cohesive sediment and the total and dissolved metal (Cd) concentrations averaged (a) over the entire period, (b) wet season (Period 1), and (c) dry season (Period 2) in 2011 and 2012. The black and gray bars represent the percentage variations of the concentrations after a 50% increase or decrease of the model input parameter from the calibrated values, respectively.

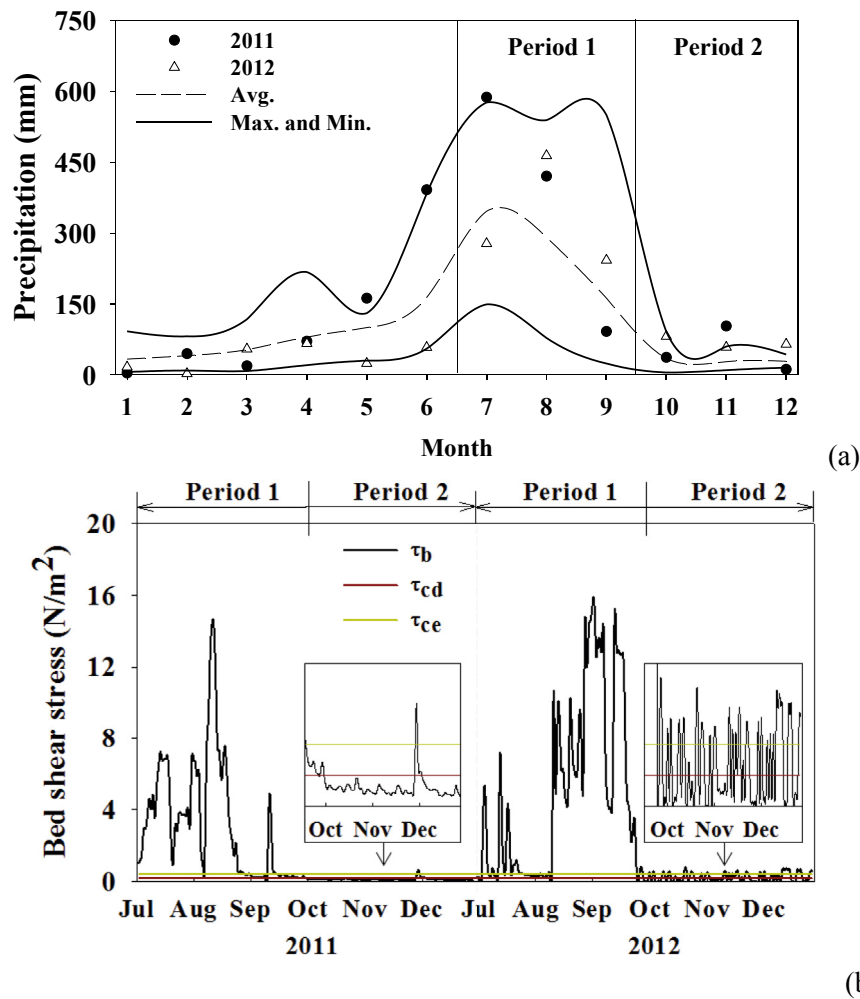


Fig. 4. (a) Precipitation patterns during the study period. Black circles and white triangles refer to the monthly total precipitation in 2011 and 2012, respectively. The lines indicate the maximum and minimum precipitation over 10 years (2001–2010), and the dashed line indicates the average value over 10 years. (b) Variation in the simulated bed shear stress with the critical deposition and erosion stresses.

contrast, the sensitivity rankings for dissolved Cd concentrations were more dependent on the rainfall variability. Specifically, the critical erosion stress, suspended sediment-water Cd partitioning coefficient, and critical deposition stress were the most influential parameters over the entire study period, wet and low flow seasons, respectively.

The absolute means (μ^*) and standard deviations (σ) of the input parameters, after the application of Morris screening method, are presented in Fig. 5a–c. A high absolute mean value indicates a greater parameter effect on the model output, while a high standard deviation suggests non-linear model response to parameter changes or significant interactive effects with other parameters (Campolongo et al., 2007). The two statistics can be combined into one single value, using the Euclidean distance $= \sqrt{(\mu^*)^2 + \sigma^2}$, to obtain the order of importance of the parameters. Thus, a high Euclidean distance for a particular parameter shows both greater parameter influence on model outputs and presence of non-linearity and/or interactions with the rest parameters (Table 4).

Counter to the local sensitivity analysis, the Morris screening method identified that the sensitivity ranking of settling velocity, critical deposition and erosion stresses for the suspended sediment concentration differed depending on the flow regime simulated (Fig. 5a). Specifically, the critical erosion stress was the most influential parameter when examining the entire simulation period

and the low flow season (Period 2). By contrast, the settling velocity appears to be the most sensitive parameter during the high flow conditions (Period 1). It is also interesting to note that the absolute mean and standard deviation values of the settling velocity did not vary with the flow regimes, whereas those of the critical erosion stress were significantly changed. With the OAT method, even though the ranking was not changed, the degree of sensitivity of the critical erosion stress varied to a greater degree relative to the settling velocity (Table 3). The average sensitivity of the critical erosion stress changed from 14.86 to 4.79% between low and high flow conditions, whereas the corresponding values for the settling velocity changed from 5.72 to 2.33%. Gamerith et al. (2013) reported that the absolute mean and standard deviation values could be altered by the simulated river flow conditions, and therefore the Morris screening method provides a reliable overview of the relative importance of uncertain factors.

The results of the sensitivity analysis with respect to total Cd concentration in water using the Morris screening method differed from those of the local sensitivity analysis (Fig. 5b). The Cd partitioning coefficient between sediment bed and water column was the most influential parameter with the former method, while the OAT approach gave more emphasis on the critical erosion stress (Table 4). The difference of the results between the two methods may stem from the wide range assigned to Cd partitioning

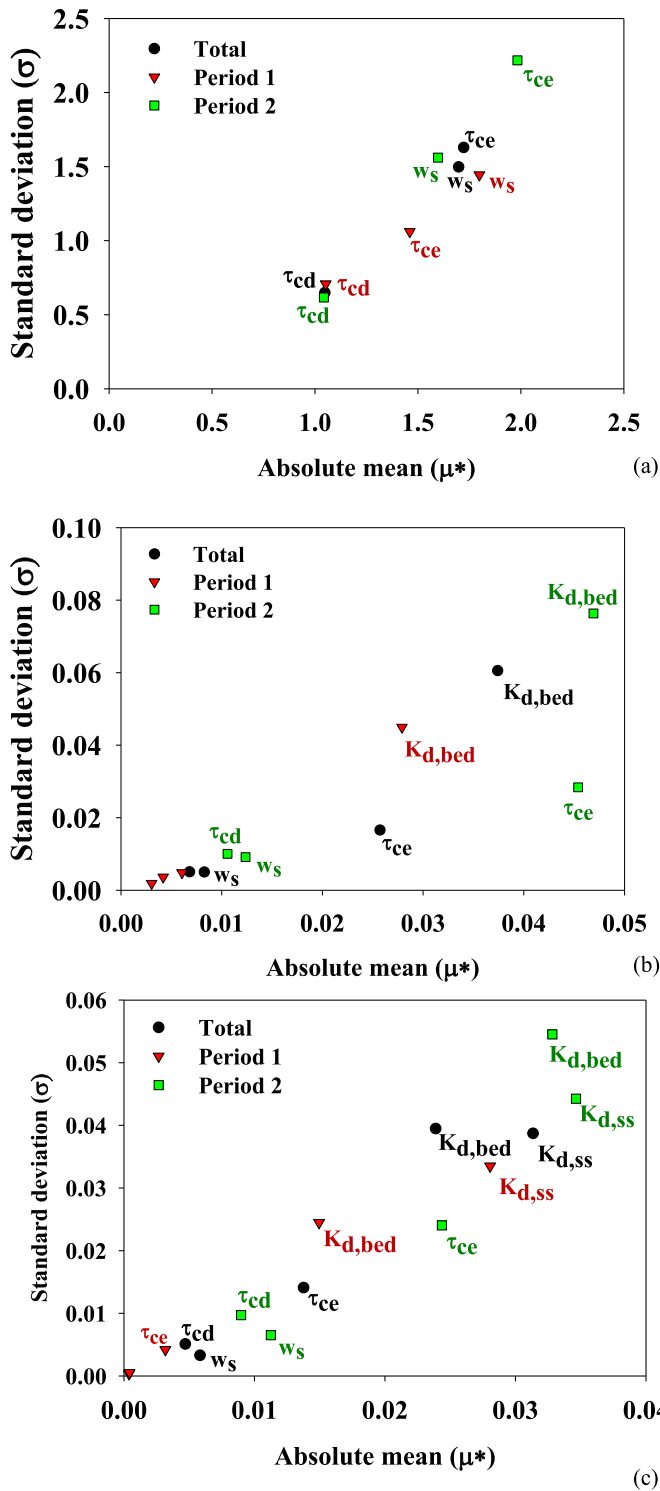


Fig. 5. Results of Morris screening method for (a) the cohesive sediment concentration, (b) the total metal concentration, and (c) the dissolved metal concentration obtained using the Morris screening method. The black circle, red inverted triangle, and green squares represent the values averaged over the entire period, Period 1, and Period 2, respectively. (For interpretation of the references to colour in this figure legend, the reader is referred to the web version of this article.)

coefficient between sediment bed and water (10–6 to 100) as well as the likelihood of non-linear model response or significant interactions among model parameters (Neumann, 2012). Sun et al. (2012) compared the influence of input parameters using several

sensitivity analysis methods and found that the sensitivity ranking of the relative volume of the slow flow response to nitrate concentration was in the fourth place using local sensitivity analysis, but it was the most important parameter with the Morris screening method. In a similar manner, the sensitivity parameter ranking with dissolved Cd concentrations varied among the simulation period examined (Fig. 5c). The sediment bed-water partitioning coefficient was the most influential parameter when low flow conditions prevailed. However, the Cd partitioning coefficient between suspended sediment and water was the most sensitive parameter during high flow conditions, which is in agreement with the OAT method.

3.2. Uncertainty analysis

The error bands of the predicted total suspended sediment concentrations when propagating the prior parameter uncertainty through the model are presented in Table 5 and Fig. 6. Most observed data were included within the uncertainty band of the prior predictive distribution, but this error zone was excessively broad and therefore uninformative in the context of environment management. To address this problem, the model was updated with the total suspended sediment concentrations measured in two locations (TS-1 and TS-2) during 2011 and 2012. This updating exercise was repeated twice; we first used collectively all data from the entire study period and then separately the subset of data collected from the low flow season (see following discussion). Fig. 7 shows the comparison between prior and posterior distributions, according to the number of iterations used to explore the parameter space. In Table 6, we also summarize the posterior average and standard deviation values derived for the settling velocity, critical deposition, and erosion stresses. The delineation of the probability distributions of the cohesive sediment parameters significantly improved with as the iteration number increased; especially when we used greater than 1000 parameter sets. To generate more precise estimates of the parameter posteriors with the Bayesian Monte Carlo method, a larger number of iterations is required; otherwise, the parameter distributions can appear to be irregular (Dilks et al., 1992; Qian et al., 2003). In this regard, when the iteration number was 5,000, we found that the posterior distributions of the settling velocity and critical deposition stress became right-skewed, i.e., the mass of the distribution is concentrated on small values while the right tail is longer.

The posterior uncertainty bands of the predicted total suspended sediment concentrations were not greatly changed in regard to their (average and maximum) width, when the entire data set was used to update the model (Table 5). The existence of large uncertainties in estimating the total suspended sediment concentrations may be explained by the fact that the measured data reflected both cohesive and non-cohesive sediment. As previously mentioned, the public data available for suspended solids in the water column are summarized as the total suspended sediment values, and therefore their use was not appropriate to update the cohesive sediment parameters. To overcome this problem, we developed another strategy to use the observed data and more effectively update the cohesive sediment parameters. The suspended non-cohesive sediment increases with heavy rainfall and high flow rate. The amount of cohesive and non-cohesive sediments was around 10% and 90% in the high flow season, but switched to 88% and 12% when low flow conditions prevailed (KME, 2010; KME, 2011b, 2012b). Therefore, data from the former period would contain little information for estimating the posteriors of the cohesive sediment parameters.

Model updating based on data collected from the low-flow season allowed obtaining parameter posteriors and predictive

Table 4
Euclidean distance of the parameters using the Morris screening method. Bold numbers indicate the most sensitive parameter in each period.

Input parameter	Cohesive sediment concentration			Total metal concentration			Dissolved metal concentration		
	Total	Period 1	Period 2	Total	Period 1	Period 2	Total	Period 1	Period 2
	Settling velocity (w_s)	2.26	2.31	2.23	0.010	0.006	0.015	0.007	0.001
Critical deposition stress (τ_{cd})	1.23	1.27	1.21	0.008	0.004	0.015	0.007	0.001	0.013
Critical erosion stress (τ_{ce})	2.37	1.81	2.98	0.031	0.008	0.054	0.020	0.005	0.034
Cd partitioning coefficient between suspended sediment and water ($K_{d,ss}$)	—	—	—	—	—	—	0.050	0.044	0.056
Cd partitioning coefficient between sediment bed and water ($K_{d,bed}$)	—	—	—	0.071	0.053	0.090	0.046	0.029	0.064

Table 5
Average and maximum uncertainty bands of total suspended sediment concentrations of the prior and posterior predictive distributions when the entire dataset or data collected during the Period 1 and 2 were used for updating the model. TS-1 and TS-2 indicate the monitoring points as shown in Fig. 1.

	TS-1 (Geumbon G)				TS-2 (Geumbon H)			
	Prior	Posterior			Prior	Posterior		
		Total	Period 1	Period 2		Total	Period 1	Period 2
Avg. band width	9.12	9.02	9.88	0.50	10.29	11.22	11.08	1.89
Max. band width	90.32	92.54	98.89	4.20	44.21	38.46	42.28	7.35

distributions that were characterized by significantly reduced standard deviations; Fig. 7b–1, b–2, b–3 & Table 6b. In particular, when using 5000 parameter samples, we found that the uncertainties of settling velocity and critical deposition stress were reduced and predominantly became right-skewed. The same pattern held true for the critical erosion stress which became left-skewed, i.e., greater likelihood was assigned to the upper end of the values ascribed to that parameter. When inspecting the posterior predictive distributions of the total suspended sediment concentrations, we can infer that the model updating with observed data from low flow conditions improved the performance and reduced

the corresponding uncertainties (Fig. 7b & Table 5). Importantly, not only did the uncertainties of the total suspended sediment concentrations in Period 2 decrease, but also those in Period 1. In other words, the uncertainties of the total suspended sediment concentrations for the entire period were significantly reduced. On the other hand, when observed data solely from high-flow conditions were used for calculating the likelihood function, the parameter posteriors and the uncertainty bands of the predictive distributions of the total suspended sediment concentrations remained practically unaltered (Figs. S4–S5). Therefore, one may conclude that the observed data derived during the low rainfall

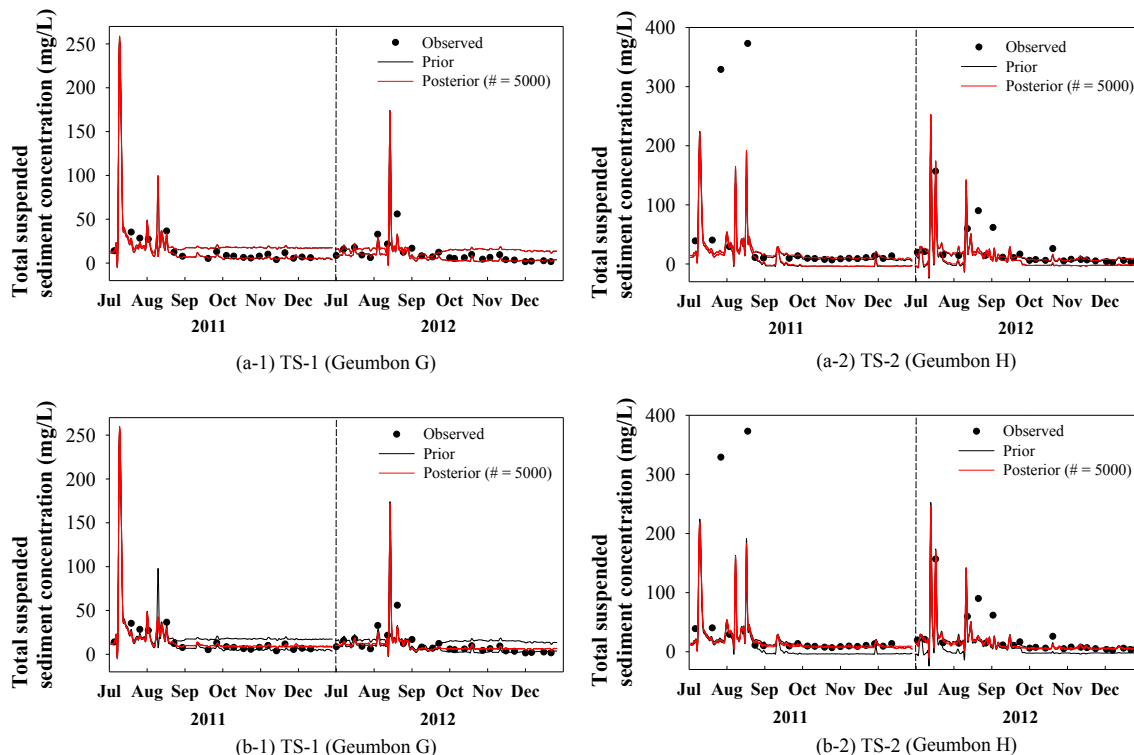


Fig. 6. Prior and posterior predictive distributions of total suspended sediment concentrations (a-1)–(a-2) when the entire dataset or (b-1)–(b-2) data collected only during the Period 2 were used for updating the model.

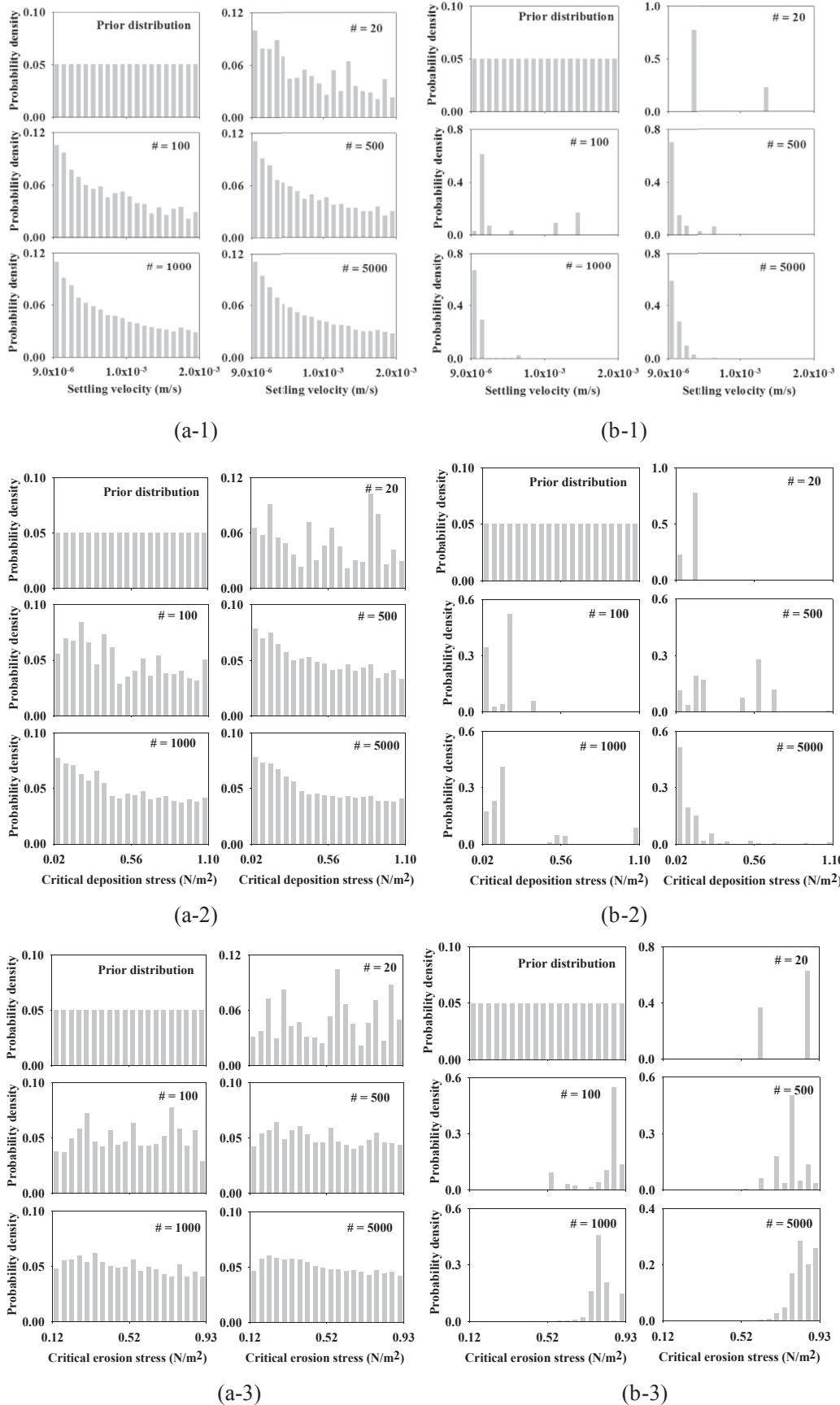


Fig. 7. Prior and posterior parameter distributions according to the iteration numbers (a-1)-(a-3) when the entire dataset or (b-1)-(b-3) data collected only during the Period 2 were used for updating the model. (1) settling velocity, (2) critical deposition stress, and (3) critical erosion stress.

Table 6a

(a): Average and standard deviation values obtained from the posterior parameter distributions when total suspended sediment concentration collected during the entire study period were used for updating the model.

Iteration	Settling velocity (m/s)		Critical deposition stress (N/m ²)		Critical erosion stress (N/m ²)	
	Avg. ($\times 10^{-4}$)	Std. ($\times 10^{-4}$)	Avg. ($\times 10^{-1}$)	Std. ($\times 10^{-1}$)	Avg. ($\times 10^{-1}$)	Std. ($\times 10^{-1}$)
20	8.05	5.73	5.29	3.28	5.38	2.30
100	7.73	5.60	4.92	3.17	5.23	2.29
500	7.74	5.74	4.88	3.15	5.08	2.33
1000	7.75	5.74	4.92	3.17	5.02	2.32
5000	7.72	5.73	4.90	3.19	5.02	2.33

Table 6b

(b): Average and standard deviation values obtained from the posterior parameter distributions when total suspended sediment concentration collected during the low-flow season (Period 2) were used for updating the model.

Iteration	Settling velocity (m/s)		Critical deposition stress (N/m ²)		Critical erosion stress (N/m ²)	
	Avg. ($\times 10^{-4}$)	Std. ($\times 10^{-4}$)	Avg. ($\times 10^{-1}$)	Std. ($\times 10^{-1}$)	Avg. ($\times 10^{-1}$)	Std. ($\times 10^{-1}$)
20	5.96	4.25	1.08	0.48	7.64	1.16
100	4.94	4.95	1.62	1.21	8.27	1.09
500	1.17	1.68	3.62	2.45	7.68	0.68
1000	0.99	1.08	2.37	2.85	8.03	0.64
5000	1.18	0.91	1.28	1.59	8.37	0.57

period with high amount of cohesive sediments possess high information value, resulting in a substantial uncertainty reduction in the cohesive sediment parameters relative to the entire data set. Thus, greater data sample sizes do not necessarily entail greater information content for model updating, as there are many factors that determine their suitability to effectively guide model parameterization.

The probability distributions of the cohesive sediment parameters and the metal partitioning coefficient between suspended sediment and water column were jointly updated using total metal concentrations measured at location M (Fig. 1). It is interesting to note that the parameter posteriors remained practically unaltered (see critical erosion stress in Fig. 8a & and rest parameters in Fig. S6). When the entire observed data set was used to update the model, the prior and posterior uncertainty bands captured the measured total Cd concentrations from 2011, whereas the observed data from 2012 differed significantly from the corresponding predictions (Fig. 8b). Regarding the latter finding, we hypothesize that this discrepancy may stem from the model structural error, e.g., missing key adsorption processes or misspecification of boundary conditions, which cannot be quantified by the present parameter uncertainty analysis exercise (Refsgaard et al., 2006; Matott et al., 2009; Ramin and Arhonditsis, 2013). For example, the effects of algal blooms and the spatial and temporal variation of organic sediment content are not explicitly considered by the present model. In Korea, there are many reports about the occurrence of algal blooms, especially when the water temperature rises, which

induce biosorption of heavy metals from aqueous solutions (Abdel-Aty et al., 2013; Tekile et al., 2015). In addition, the content of organic matter can significantly modulate the degree of metal adsorption onto sediments (Lee et al., 1996). For illustrative purposes, we also updated the model using total metal concentration data solely from 2011. The shape of the derived posterior for the critical erosion stress was significantly changed and clearly left-skewed (Fig. 9a & Fig. S7). The average value of the posterior critical erosion stress was 0.726 N/m², which was similar to the value obtained when total suspended sediment concentrations from low flow season were used to update the model. By contrast, the other parameters were not updated in the same fashion. Additionally, the uncertainty band of the posterior predictive distribution, when observed data from 2011 were used, was smaller than the error estimates from the entire data set (Fig. 9b & Table 7).

As a final exercise, we updated the model using dissolved metal concentrations from 2011 to 2012, while the parameter vector comprised the cohesive sediment parameters and Cd partitioning coefficient between suspended sediment and water column, and Cd partitioning coefficient between sediment bed and water column. The posterior of the suspended sediment-water partitioning coefficient, the most sensitive parameter based on the Morris screening method, was dramatically changed (Fig. 10a). The average posterior value was 0.0827 L/mg, which was a little higher than the calibrated value. However, except from the right-skewed posterior for critical erosion stress, the rest parameters were not updated and remained fairly flat (Fig. S8). The predicted average dissolved metal

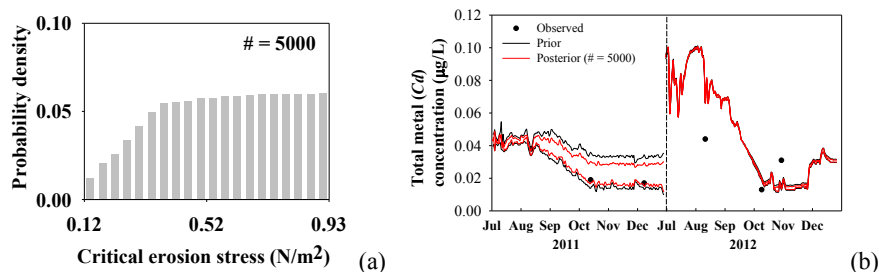


Fig. 8. (a) Posterior distribution of the critical erosion stress and (b) prior and posterior predictive distributions of total metal (Cd) concentrations when the entire dataset was used for updating the model.

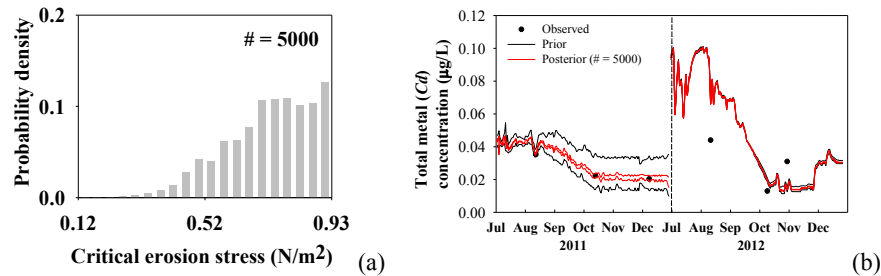


Fig. 9. (a) Posterior distribution of the critical erosion stress and (b) prior and posterior predictive distributions of total metal (Cd) concentrations when data collected in 2011 were used for updating the model.

concentrations were in better agreement with the observed data relative to the original calibration (Fig. 10b), although the average and maximum uncertainty bands slightly increased (Table 7). Relative to the calibration that revolved around the total suspended sediment concentrations though, neither the quantity (number of observations) nor the value of information characterizing the metal concentrations allowed gaining insights into the cohesive sediment parameter values. The total suspended sediment dataset comprised 91 measurements at two monitoring points (TS-1, TS-2 in Fig. 1), while the Cd concentrations were only measured 6 times at one monitoring point (M in Fig. 1) within a 2-yr period. The metal partitioning coefficient between sediment bed and water column, which was the most influential parameter to the predicted total metal concentration based on the Morris screening method, was not updated by the observed data. In addition, the settling velocity and critical deposition stress were not updated by the observed metal concentration, suggesting that the available data likely do not contain all of the information needed to constrain these parameters (Kanso et al., 2005).

4. Conclusions-future perspectives

Environmental models are subject to substantial uncertainty contributed from a variety of sources, including model structural error, input and calibration data uncertainty, and model parameter uncertainty. Uncertainty analysis refers to evaluating all these sources of potential bias during the application of a model in order to ensure that any conclusions drawn are robust. Sensitivity analysis is typically considered as the first step to accomplish this assessment. Nonetheless, despite the compelling reasons to becoming an integral part of the model development process, a thorough sensitivity analysis entails an excessively high number of model runs that was historically deemed an impediment for its broader application (Arhonditsis and Brett, 2004; Sun et al., 2012). The advent of fast computing though coupled with the development of sophisticated sensitivity analysis techniques has spawned a

number of peer-reviewed studies that aimed to shed light on different facets of environmental models (Saltelli, 2008). Parameter identification has been a focal point in environmental modeling research in an effort to optimize complexity and achieve parsimonious model constructs (Freni et al., 2011). In this study, we focused on a critical component of micropollutant modeling concerning the parameterization of the processes that modulate the exchange of contaminants between sediment and water column. We first used an OAT method aiming to investigate the response of output variables to fractional changes of input parameters (Saltelli, 2008), followed by the Morris screening method that relies on a local sensitivity measure, the elementary effect, but the final evaluation is obtained by averaging these elementary effects computed at different points to evenly spaced values of each parameter over its entire range (Norton, 2009).

Notwithstanding their conceptual differences, the two methods (almost) consistently identified the critical erosion stress as the most influential parameter for the predictions of total suspended sediment concentrations. In case of total Cd concentration, the critical erosion stress was similarly the most sensitive parameter with the OAT method, reflecting the covariance between suspended sediments and contaminants adsorbed on their surface. However, the capacity of Morris screening method to accommodate patterns of non-linearity or interactive effects among parameters offered additional insights, highlighting the critical role of metal partitioning coefficient between sediment bed and water column. A novel “take-home-message” from our work is the importance of delineating periods of distinct flow dynamics that may profoundly shape contaminant fate and transport, such as the relative distribution of the total suspended sediment pool between cohesive and non-cohesive material. According to this classification, the variability associated with the settling velocity during high flow conditions can be another influential factor in regard to the predictions of total suspended particles. In a similar manner, the assumptions made about the metal partitioning coefficient between suspended sediments and water column are strongly related to model outputs for dissolved Cd concentration. By contrast, when focusing on river flow regime associated with dry conditions, our analysis gave greater weight to the sediment bed-water partitioning coefficient for effectively predicting the amount of dissolved-phase metals.

Quantifying the uncertainty in the multidimensional parameter space of environmental models involves two critical decisions: i) selection of the sampling scheme for generating parameter input vectors, which are then evaluated with regards to the model performance, and ii) selection of the model error description, i.e., which likelihood measure should we use and why? The former decision addresses the sampling efficiency of the approach (Random sampling, Latin hypercube, Markov Chain Monte Carlo), while the latter one entails conceptual dilemmas involving the

Table 7

Average and maximum uncertainty bands of total and dissolved metal concentrations of the prior and posterior predictive distributions when the entire dataset or data collected only in 2011 were used for updating the model.

	Total metal concentration			Dissolved metal concentration	
	Prior	Posterior		Prior	Posterior
		Total	2011		Total
Avg. band width	0.0083	0.0049	0.0012	0.0247	0.0276
Max. band width	0.0257	0.0185	0.0116	0.0661	0.0739

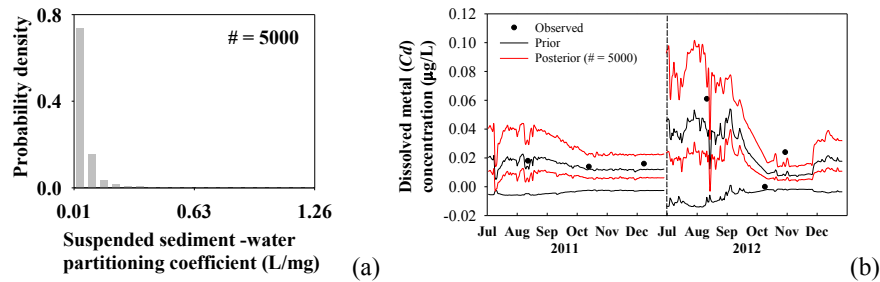


Fig. 10. (a) Posterior distribution of the Cd suspended sediment-water partitioning coefficient and (b) prior and posterior predictive distributions of the dissolved metal (Cd) concentrations.

selection of generalized (e.g., Root Mean Square Error, Reliability Index, U-uncertainty) or purely probabilistic (e.g., Normal, Lognormal or Poisson error) likelihood functions that can significantly alter the results (Qian et al., 2003; Arhonditsis et al., 2008a,b). In this study, we opted for a formal (Gaussian) likelihood coupled with a Latin hypercube sampling scheme, which allowed drawing samples uniformly from plausible parameter ranges. When using data collected from the low flow season, our Bayesian Monte Carlo approach led to parameter posteriors and predictive distributions that were characterized by significantly reduced standard deviations. The value of information of suspended sediment data dominated by cohesive material was clearly sufficient to effectively delineate the posteriors of the cohesive sediment parameters, such as settling velocity, critical deposition stress, and critical erosion stress. Given also the low number (3) of parameters considered in this exercise, it took approximately 1000–5000 runs to reach a satisfactory degree of updating. Following the same reasoning though, both the quantity (sampling frequency) and value of information of total and dissolved Cd concentrations were not adequate to constrain a calibration vector that was still fairly small (4–5 parameters). Given that micropollutant models typically contain a significantly higher number of parameters, the latter result casts doubt on the ability of the present uncertainty analysis framework to elucidate their uncertainty patterns.

The efficiency of the Bayesian Monte Carlo strategy was challenged in the modeling literature with respect to the parameter priors, sampling schemes, and model error specifications typically used (Qian et al., 2003). One of the main criticisms is that the vast majority of Bayesian Monte Carlo applications in the literature resembled likelihood-based inference than true Bayesian process, as they used uniform priors with wide ranges assigned to each unknown parameter. Counter to what Bayes' theorem stipulates though, this practice treats the posterior parameter distribution as proportional to the likelihood function (and not to the product of the prior distribution and the likelihood function). The evaluation of the posterior is merely done by substituting the prior selected parameter samples into the likelihood function. Further, this strategy can misrepresent regions of high model likelihood; especially, when the joint prior parameter distribution is very wide or the parameters are highly correlated and thus the volume of the important region of the posterior parameter space can be small compared to the volume of the sampled space (Qian et al., 2003; Arhonditsis et al., 2008a). One way to maximize the efficiency of our sampling strategy is to formulate informative prior distributions from existing scientific knowledge, past experience, and results from preliminary exploratory analysis. With this configuration, we may be able to focus on subregions of the parameter space, where there is evidence for higher likelihood of realistic reproduction of the observed contaminant spatiotemporal

trends. Even more effective for future applications could be the implementation of Markov chain Monte Carlo sampling schemes; an adaptive method specifically designed to sample directly from the posterior distribution and to converge to the most probable region (Gelman et al., 2013). Generally, the Markov chain Monte Carlo procedure provides a convenient means to efficiently sample the parameter space of varying degree of complexity models, while treating stochastically other inputs, e.g., initial conditions, boundary conditions (Gilks et al., 1998). Another problem with the typical Bayesian Monte Carlo applications is the specification of the model error term σ^2 . In this study, we did not adopt the common strategy to assign an *a priori* value, based on the statistical analysis of field sampling data and/or laboratory measurement errors (Dilks et al., 1992). Because of the profound bias that could be introduced with this strategy (Qian et al., 2003), we opted for the estimation of the standard deviation of the series of residuals between our observations and the corresponding model predictions, assuming the errors are homoscedastic. The latter assumption though may not hold true, and thus the best way to improve the present uncertainty analysis framework is to consider the error term as an additional parameter to be estimated during the Bayesian inference process (Arhonditsis et al., 2007).

The tendency to invoke complexity as a means for improving the learning capacity of our models is primarily prompted by the need to address environmental management problems that often involve complex policy decisions. As the articulation level of micropollutant models continues to grow, an emerging imperative is the development of novel uncertainty analysis techniques to rigorously assess the error pertaining to model structure and input parameters (Beven, 2006). In this context, we believe that the Bayesian inference has several benefits, such as the expression of model outputs as probability distributions, the rigorous assessment of the expected consequences of different management actions, the optimization of the sampling design of monitoring programs, and the alignment with the policy practice of adaptive management, that can be particularly useful for stakeholders and policy makers when making decisions for sustainable environmental management (Arhonditsis et al., 2007).

Acknowledgments

This work was supported by the Basic Science Research Program (grant number 2012R1A1A2007689) through an NRF grant funded by MEST and by the Korean Ministry of the Environment as the Geo-Advanced Innovative Action (GAIA) Project (grant number Q1509291). Statistical analysis and interpretation were completed with the assistance of the Statistical Analysis and Consulting Center in Chungbuk National University. The metal concentration data were obtained from the reports "Monitoring of Potentially Hazardous Compounds in the 4 River Basins (Geum River Basin)".

Appendix A. Supplementary data

Supplementary data related to this article can be found at <http://dx.doi.org/10.1016/j.envsoft.2016.02.026>.

References

- Abdel-Aty, A.M., Ammar, N.S., Abdel Ghafar, H.H., Ali, R.K., 2013. Biosorption of cadmium and lead from aqueous solution by fresh water alga *Anabaena sphaerica* biomass. *J. Adv. Res.* 4, 367–374.
- Allison, J.D., Allison, T.L., 2005. Partition Coefficients for Metals in Surface Water, Soil and Waste. EPA/600/R-05/074. US Environmental Protection Agency, Washington, DC.
- Arhonditsis, G.B., Brett, M.T., 2004. Evaluation of the current state of mechanistic aquatic biogeochemical modeling. *Mar. Ecol. Prog. Ser.* 271, 13–26.
- Arhonditsis, G.B., Qian, S.S., Stow, C.A., Lamon, E.C., Reckhow, K.H., 2007. Eutrophication risk assessment using Bayesian calibration of process-based models: application to a mesotrophic lake. *Ecol. Model.* 208, 215–229.
- Arhonditsis, G.B., Perhar, G., Zhang, W., Massos, E., Shi, M., Das, A., 2008a. Addressing equifinality and uncertainty in eutrophication models. *Water Resour. Res.* 44, W01420.
- Arhonditsis, G.B., Papantou, D., Zhang, W., Perhar, G., Massos, E., Shi, M., 2008b. Bayesian calibration of mechanistic aquatic biogeochemical models and benefits for environmental management. *J. Mar. Syst.* 73, 8–30.
- Beven, K., 2006. A manifesto for the equifinality thesis. *J. Hydrol.* 320, 18–36.
- Camacho, R.A., Martin, J.L., 2013. Bayesian Monte Carlo for evaluation of uncertainty in hydrodynamic models of coastal systems. *J. Coast. Res. Spec.* 65, 886–891.
- Campolongo, F., Saltelli, A., 2000. Comparing different sensitivity analysis methods on a chemical reactions model. In: Saltelli, A., Chan, K., Scott, M. (Eds.), *Sensitivity Analysis*. John Wiley and Sons, Chichester.
- Campolongo, F., Cariboni, J., Saltelli, A., 2007. An effective screening design for sensitivity analysis of large models. *Environ. Modell. Softw.* 22, 1509–1518.
- Chu, X., Rediske, R., 2012. Modeling metal and sediment transport in a stream-wetland system. *J. Environ. Eng.* 138, 152–163.
- Dilks, D.W., Canale, R.P., Meier, P.G., 1992. Development of Bayesian Monte Carlo techniques for water quality model uncertainty. *Ecol. Model.* 62, 149–162.
- Elçi, Ş., Work, P., Hayter, E., 2007. Influence of stratification and shoreline erosion on reservoir sedimentation patterns. *J. Hydraul. Eng.* 133, 255–266.
- Franceschini, S., Tsai, C.W., 2010. Assessment of uncertainty sources in water quality modeling in the Niagara river. *Adv. Water Resour.* 33, 493–503.
- Freni, G., Mannina, G., Viviani, G., 2009. Urban runoff modelling uncertainty: comparison among Bayesian and pseudo-Bayesian methods. *Environ. Modell. Softw.* 24, 1100–1111.
- Freni, G., Mannina, G., 2010. Uncertainty in water quality modelling: the applicability of variance decomposition approach. *J. Hydrol.* 394, 324–333.
- Freni, G., Mannina, G., Viviani, G., 2011. Assessment of the integrated urban water quality model complexity through identifiability analysis. *Water Res.* 45, 37–50.
- Gamerith, V., Neumann, M.B., Muschalla, D., 2013. Applying global sensitivity analysis to the modelling of flow and water quality in sewers. *Water Res.* 47, 4600–4611.
- Gelman, A., Carlin, J.B., Stern, H.S., Rubin, D.B., 2013. *Bayesian Data Analysis*, third ed. Chapman & Hall/CRC Press.
- Gilks, W.R., Roberts, G.O., Sahu, S.K., 1998. Adaptive Markov chain Monte Carlo through regeneration. *J. Amer. Stat. Assoc.* 93, 1045–1054.
- Gunsan Regional Oceans and Fisheries Administration, 2010. A Report of Hydrological Variation on Kuem River Estuary. Korea Ministry of Land, Infrastructure and Transport, Korea.
- Hamrick, J.M., 1992. A Three-dimensional Environmental Fluid Dynamics Computer Code: Theoretical and Computational Aspects. The College of William and Mary, Virginia Institute of Marine Science. Special Report 317, 63.
- Hamrick, J.M., Wu, T.S., 1997. Computational design and optimization of the EFDC/HEM3D surface water hydrodynamic and eutrophication models. In: Delich, G., Wheeler, M.F. (Eds.), *Next Generation Environmental Models and Computational Methods*. Society of Industrial and Applied Mathematics, Philadelphia, pp. 143–156.
- Hayter, E.J., Mehta, A.J., 1983. Modeling Fine Sediment Transport in Estuaries. Report EPA-600/3-83-045. U.S. Environmental Protection Agency, Athens, GA.
- Hong, S.H., Yim, U.H., Shim, W.J., Oh, J.R., Lee, I.S., 2003. Horizontal and vertical distribution of PCBs and chlorinated pesticides in sediments from Masan Bay, Korea. *Mar. Pollut. Bull.* 46, 244–253.
- Hwang, K.N., Ryu, H.R., Chun, M.C., 2006. A study on settling properties of fine-cohesive sediments in Kuem estuary. *J. Korean Soc. Coast. Ocean Eng.* 18, 251–261.
- Hwang, K.N., Yim, S.H., Ryu, H.R., 2008. Analyses on local-seasonal variations of erosional properties of cohesive sediments in Kuem estuary. *J. Korean Soc. Civ. Eng.* 28, 125–135.
- Ji, Z., 2008. *Hydrodynamics and Water Quality: Modeling Rivers, Lakes, and Estuaries*, first ed. Wiley, New York.
- Ji, Z., Hamrick, J., Pagenkopf, J., 2002. Sediment and metals modeling in shallow river. *J. Environ. Eng.* 128, 105–119.
- Kanso, A., Chebbo, G., Tassin, B., 2005. Bayesian analysis for erosion modelling of sediments in combined sewer systems. *Water Sci. Technol.* 52, 135–142.
- Kim, T.I., 2002. Hydrodynamics and Sedimentation Processes in the Kuem River Estuary, West Coast of Korea. Ph.D. Thesis. Sungkyunkwan Univ., p. 204.
- KME, 2010. The Prediction of Riverbed Change, Sediments and Dredging Period after Building Hydraulic Structures in the Geum River. Korea Ministry of Environment, Korea.
- KME, 2011a. Monitoring of Potentially Hazardous Compounds in the 4 River Basins (Geum River Basin) and Risk Assessment. Korea Ministry of Environment, Korea.
- KME, 2011b. The Investigation of Sedimentary Environment Near Diversion Dam for Developing Management Practice and Protocols. Korea Ministry of Environment, Korea.
- KME, 2014. Water Information System. Water quality database. <http://water.nier.go.kr/main/mainContent.do>.
- Krysanova, V., Hattermann, F., Wechsung, F., 2007. Implications of complexity and uncertainty for integrated modelling and impact assessment in river basins. *Environ. Modell. Softw.* 22, 701–709.
- K-Water, 2014. The Geum River Flood Control Office. Hydrological database. <http://www.geumriver.go.kr/html/index.jsp>.
- Lee, S., Allen, H.E., Huang, C.P., Sparks, D.L., Sanders, P.F., Peijnenburg, W.J.G.M., 1996. Predicting soil-water partition coefficients for cadmium. *Environ. Sci. Technol.* 30, 3418–3424.
- Liu, W., Chen, W., Chang, Y., 2012. Modeling the transport and distribution of lead in tidal Keelung river estuary. *Environ. Earth Sci.* 65, 39–47.
- Maa, J., Kwon, J., Hwang, K., Ha, H., 2008. Critical bed-shear stress for cohesive sediment deposition under steady flows. *J. Hydraul. Eng.* 134, 1767–1771.
- Marsili-Libelli, S., Giusti, E., 2008. Water quality modelling for small river basins. *Environ. Modell. Softw.* 23, 451–463.
- Matthies, M., Berding, V., Beyer, A., 2004. Probabilistic uncertainty analysis of the European Union System for the evaluation of substances multimedia regional distribution model. *Environ. Toxicol. Chem.* 23, 2494–2502.
- Matott, L.S., Babendreier, J.E., Purucker, S.T., 2009. Evaluating uncertainty in integrated environmental models: a review of concepts and tools. *Water Resour. Res.* 45, W06421.
- Mehta, A.J., 1986. Characterization of Cohesive Sediment Properties and Transport Processes in Estuaries, in Anonymous Estuarine Cohesive Sediment Dynamics. Springer-Verlag, pp. 290–325.
- Moldovan, Z., 2006. Occurrences of pharmaceutical and personal care products as micropollutants in rivers from Romania. *Chemosphere* 64, 1808–1817.
- Morris, M.D., 1991. Factorial sampling plans for preliminary computational experiments. *Technometrics* 33, 161–174.
- National Research Council, 2001. *Assessing the TMDL Approach to Water Quality Management*. National Academy Press, Washington, DC.
- Neumann, M.B., 2012. Comparison of sensitivity analysis methods for pollutant degradation modelling: a case study from drinking water treatment. *Sci. Total Environ.* 433, 530–537.
- Norton, J.P., 2009. Selection of Morris trajectories for initial sensitivity analysis. In: 15th IFAC Symposium on System Identification (SYSID 2009). St. Malo, France.
- Ongley, E.D., Krishnappan, B.G., Droppo, I.G., Rao, S.S., Maguire, R.J., 1992. In: Hart, B.T., Sly, P.G. (Eds.), *Cohesive Sediment Transport: Emerging Issues for Toxic Chemical Management*. Springer Netherlands, pp. 177–187.
- Onishi, Y., Graber, H.C., Trent, D.S., 1993. Preliminary Modeling of Wave-enhanced Sediment and Contaminant Transport in New Bedford Harbor, in Anonymous Nearshore and Estuarine Cohesive Sediment Transport. American Geophysical Union, pp. 541–557.
- Qian, S.S., Stow, C.A., Borsuk, M.E., 2003. On Monte Carlo methods for Bayesian inference. *Ecol. Model.* 159, 269–277.
- Ramin, M., Arhonditsis, G.B., 2013. Bayesian calibration of mathematical models: optimization of model structure and examination of the role of process error covariance. *Ecol. Inf.* 18, 107–116.
- Refsgaard, J.C., Nilsson, B., Brown, J., Klauer, B., Moore, R., Bech, T., Vurro, M., Blind, M., Castilla, G., Tsanis, I., Biza, P., 2005. Harmonised techniques and representative river basin data for assessment and use of uncertainty information in integrated water management (HarmoniRiB). *Environ. Sci. Policy* 8, 267–277.
- Refsgaard, J.C., van der Sluijs, J.P., Brown, J., van der Keur, P., 2006. A framework for dealing with uncertainty due to model structure error. *Adv. Water Resour.* 29, 1586–1597.
- Reichert, P., 1997. On the necessity of using imprecise probabilities for modelling environmental systems. *Water Sci. Tech.* 36, 149–156.
- Ruark, M., Niemann, J., Greimann, B., Arabi, M., 2011. Method for assessing impacts of parameter uncertainty in sediment transport modeling applications. *J. Hydraul. Eng.* 137, 623–636.
- Ryu, H.R., Lee, H.S., Hwang, K.N., 2006. The quantitative estimation of erosion rate parameters for cohesive sediments from Keum estuary. *J. Korean Soc. Coast. Ocean Eng.* 18, 283–293.
- Saltelli, A., 2008. *Global Sensitivity Analysis: the Primer*. John Wiley & Sons, Ltd, Chichester.
- Saltelli, A., Annoni, P., 2010. How to avoid a perfunctory sensitivity analysis. *Environ. Modell. Softw.* 25, 1508–1517.
- Saltelli, A., Ratto, M., Andres, T., Campolongo, F., Cariboni, J., Gatelli, D., Saisana, M., Tarantola, S., 2007. *Introduction to Sensitivity Analysis*, in Anonymous Global Sensitivity Analysis. The Primer. John Wiley & Sons, Ltd, pp. 1–51.
- Saltelli, A., Tarantola, S., Campolongo, F., Ratto, M., 2002. The Screening Exercise, in Anonymous Sensitivity Analysis in Practice. John Wiley & Sons, Ltd, pp. 91–108.
- Sauve, S., Hendershot, W., Allen, H.E., 2000. Solid-solution partitioning of metals in contaminated soils: dependence on pH, total metal burden, and organic matter.

- Environ. Sci. Technol. 34, 1125–1131.
- Shen, Z., Chen, L., Chen, T., 2012. Analysis of parameter uncertainty in hydrological and sediment modeling using GLUE method: a case study of SWAT model applied to three gorges reservoir region, China. *Hydrol. Earth Syst. Sci.* 16, 121–132.
- Shen, Z., Hong, Q., Yu, H., Niu, J., 2010. Parameter uncertainty analysis of non-point source pollution from different land use types. *Sci. Total Environ.* 408, 1971–1978.
- Sohn, M., Small, M., Pantazidou, M., 2000. Reducing uncertainty in site characterization using Bayes Monte Carlo methods. *J. Environ. Eng.* 126, 893–902.
- Sommerfreund, J., Arhonditsis, G.B., Diamond, M.L., Frignani, M., Capodaglio, G., Gerino, M., Bellucci, L., Giuliani, S., Mugnai, C., 2010. Examination of the uncertainty in contaminant fate and transport modeling: a case study in the Venice lagoon. *Ecotoxicol. Environ. Saf.* 73, 231–239.
- Sun, X.Y., Newham, L.T.H., Croke, B.F.W., Norton, J.P., 2012. Three complementary methods for sensitivity analysis of a water quality model. *Environ. Modell. Softw.* 37, 19–29.
- Tekile, A., Kim, I., Kim, J., 2015. Mini-review on river eutrophication and bottom improvement techniques, with special emphasis on the Nakdong river. *J. Environ. Sci.* 30, 113–121.
- Tetra Tech, Inc., 2007. *The Environmental Fluid Dynamics Code Theory and Computation*. In: *Sediment and Contaminant Transport and Fate*, vol. 2.
- Torres, A., Bertrand-Krajewski, J.L., 2008. Evaluation of uncertainties in settling velocities of particles in urban stormwater runoff. *Water Sci. Technol.* 57, 1389–1396.
- Trento, A., Alvarez, A., 2011. A numerical model for the transport of chromium and fine sediments. *Environ. Model. Assess.* 16, 551–564.
- Vezzaro, L., Mikkelsen, P.S., 2012. Application of global sensitivity analysis and uncertainty quantification in dynamic modelling of micropollutants in stormwater runoff. *Environ. Modell. Softw.* 27–28, 40–51.
- Villaret, C., Paulic, M., 1986. *Experiments on the Erosion of Deposited and Placed Cohesive Sediments in an Annular Flume and a Rocking Flume*. Coastal and Oceanographic Dept., University of Florida. Report UFL/COEL-86/007, Gainesville, FL.
- Wang, C., Shen, C., Wang, P., Qian, J., Hou, J., Liu, J., 2013. Modeling of sediment and heavy metal transport in Taihu Lake, China. *J. Hydrodyn. Ser. B* 25, 379–387.
- Yang, C., Lung, W., Kuo, J., Lai, J., Wang, Y., Hsu, C., 2012. Using an integrated model to track the fate and transport of suspended solids and heavy metals in the tidal wetlands. *Int. J. Sediment. Res.* 27, 201–212.
- Zaramella, M., Marion, A., Packman, A.I., 2006. Applicability of the transient storage model to the hyporheic exchange of metals. *J. Contam. Hydrol.* 84, 21–35.
- Ziegler, C., Nisbet, B., 1994. Fine-grained sediment transport in Pawtuxet river, Rhode Island. *J. Hydraul. Eng.* 120, 561–576.
- Ziegler, C., Nisbet, B., 1995. Long-term simulation of fine-grained sediment transport in large reservoir. *J. Hydraul. Eng.* 121, 773–781.

**MODELING METAL-SEDIMENT INTERACTION PROCESSES:
PARAMETER SENSITIVITY ASSESSMENT AND UNCERTAINTY
ANALYSIS**

SUPPORTING INFORMATION

**Eunju Cho^a, George B. Arhonditsis^b, Jeehyeong Khim^{a*}, Sewoong Chung^{c*},
Tae-Young Heo^d**

^aSchool of Civil, Environmental and Architectural Engineering, Korea University, Seoul 136-701, Korea

^bEcological Modeling Laboratory, Department of Physical & Environmental Sciences, University of Toronto, Toronto, Ontario M1C 1A4, Canada

^cDepartment of Environmental Engineering, Chungbuk National University, Cheongju 362-763, Korea

^dDepartment of Information & Statistics, Chungbuk National University, Cheongju 362-763, Korea

*Corresponding authors:

1. Jeehyeong Khim

School of Civil, Environmental and Architectural Engineering, Korea University, Anam-dong, Seongbuk-gu, Seoul 136-701, Korea. Tel.: +82 2 3290 3318; fax: +82 2 928 7656; e-mail address: hyeong@korea.ac.kr (J. Khim)

2. Sewoong Chung

Department of Environmental Engineering, Chungbuk National University, Chungdae-ro 1, Seowon-gu, Cheongju, Chungbuk 362-763, Korea. Tel.: +82 43 261 3370; fax: +82 43 272 3370; e-mail address: schung@chungbuk.ac.kr (S.W. Chung)

INITIAL/ BOUNDARY CONDITIONS AND PARAMETER VALUES

Initial/boundary conditions and parameter values were obtained from reports published by the Korean Ministry of Environment (KME). Daily water temperatures were calculated by regression equations that captured the relationship between water temperatures at 8-day interval with flow rates and air temperatures. The regression equations of water temperature at each stream are provided in Table S1, while the comparison between measured and modeled water temperatures is shown in Fig. S3. Total suspended sediment concentrations were monitored usually once a week, and therefore daily values were not available but were calculated by a similar regression equation. Measured and modeled total suspended sediment concentrations are compared in Fig. S3. Cohesive and non-cohesive sediment concentrations were calculated based on a literature-based ratio obtained from local reports. Two sediment bed layers were simulated, and the initial ratio of cohesive and non-cohesive sediment in sediment bed was around 95% and 5% in 2011 and 40% and 60% in 2012, respectively. Porosity of sediment bed and sediment specific gravity were set equal to 0.4 and 2.65, respectively. Metal concentrations were monitored three times per year as shown in Table S2. The diffusion coefficient of metals between sediment bed and water interface was set equal to $5.7 \times 10^{-10} \text{ m}^2/\text{s}$. The assumption with respect to the metal adsorption was that metals are adsorbed solely on the surface of cohesive sediments.

Table S1: Regression equations of water temperature (T_w , °C) as a function of air temperature (T_a , °C) and flow rate (Q , m³/s).

	Equation
Main stream	$T_w = 6.333 + 0.657T_a - 0.0072Q$ ($r^2 = 0.815$)
Gap stream	$T_w = 8.366 + 0.692T_a - 0.0065Q$ ($r^2 = 0.926$)
Miho stream	$T_w = 4.929 + 0.812T_a - 0.0071Q$ ($r^2 = 0.931$)

Table S2: Measured total *Cd* concentrations (µg/L) in Geum River.

	2011			2012		
	Aug.12-14	Oct.14-18	Dec.10-12	Aug.13-16	Oct.12-18	Dec.11.02
Main stream	0.014	0.009	0.011	0.107	0	0.15
Gap stream	0.017	0.021	0.006	0.076	0.007	0.026
Miho stream	0.013	0.042	0.016	0.091	0.02	0.024

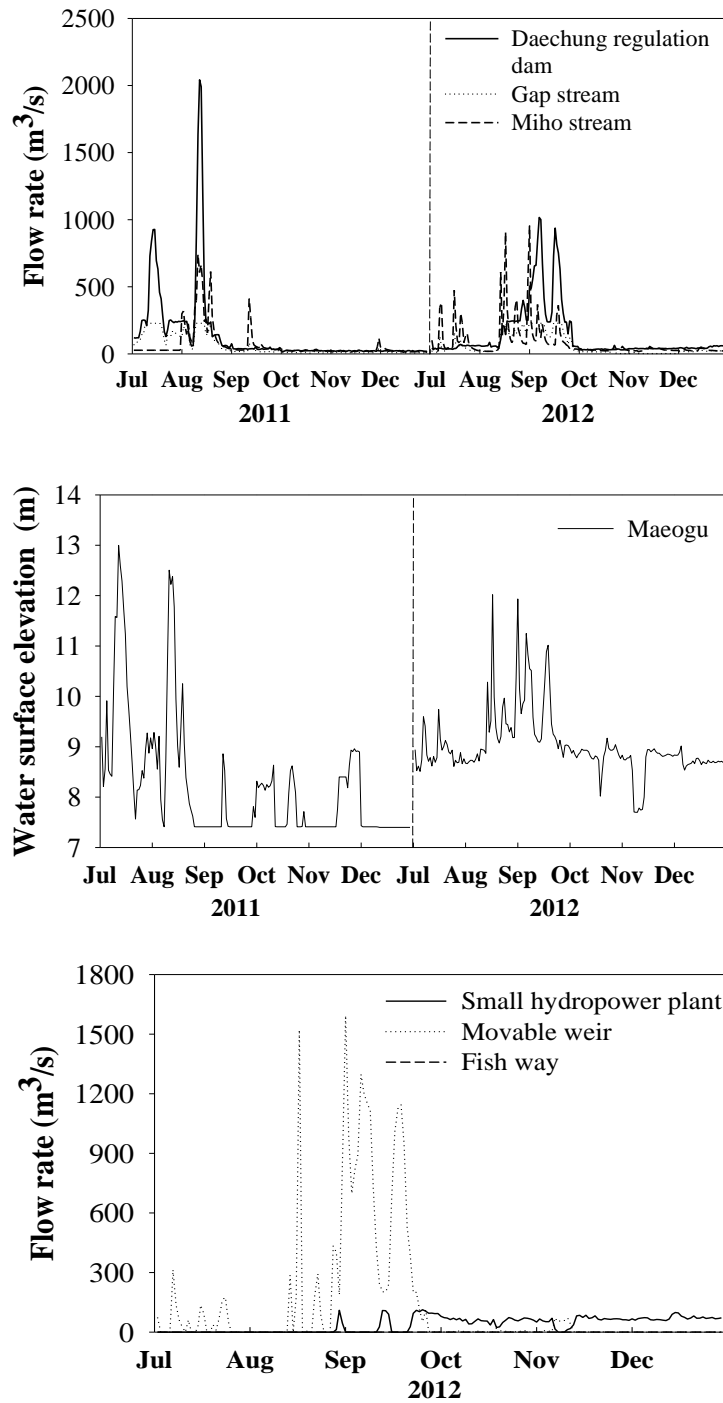
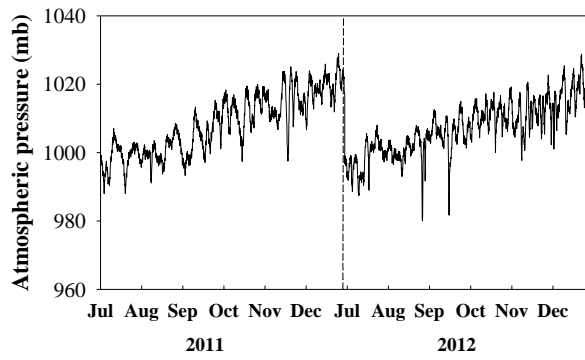
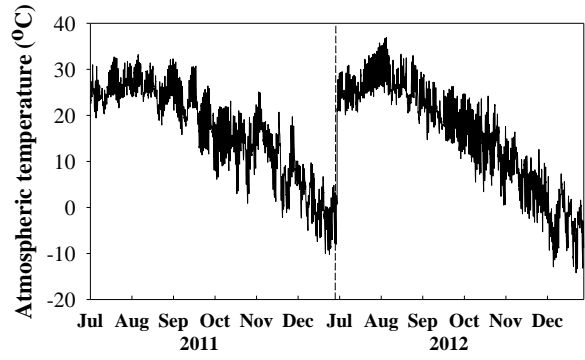


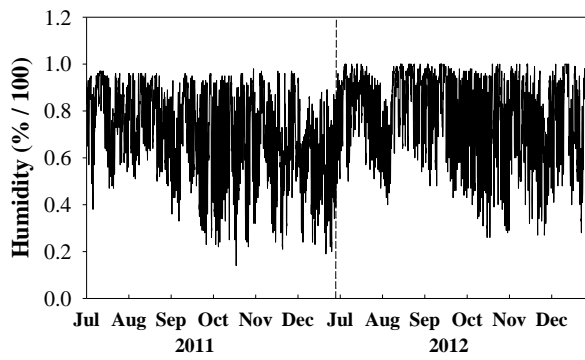
Fig. S1: Boundary conditions for hydrodynamics. The main stream flows from Daechung Regulation Dam to Maeogu that is fed by two tributaries, Gap stream, and Miho stream.



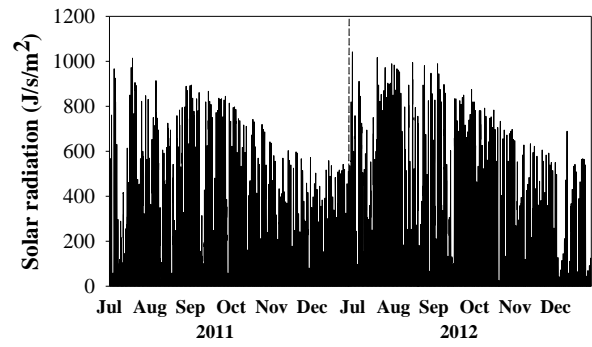
(a)



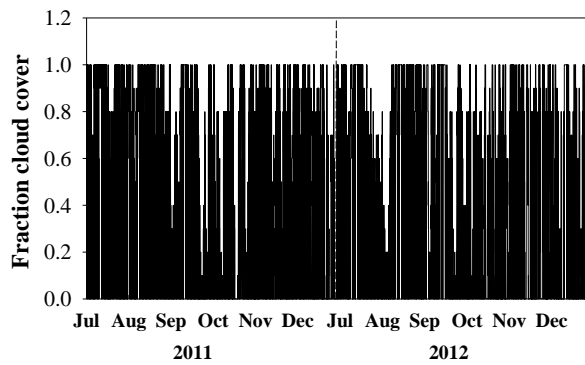
(b)



(c)

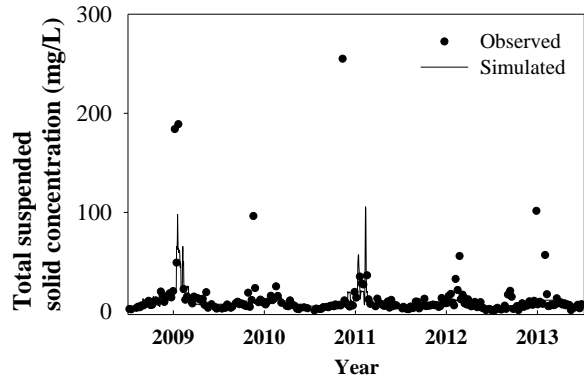
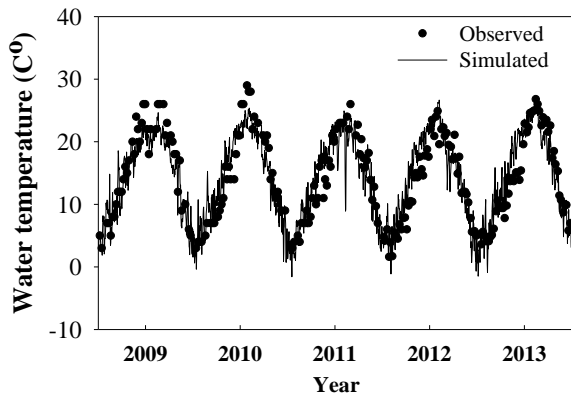


(d)

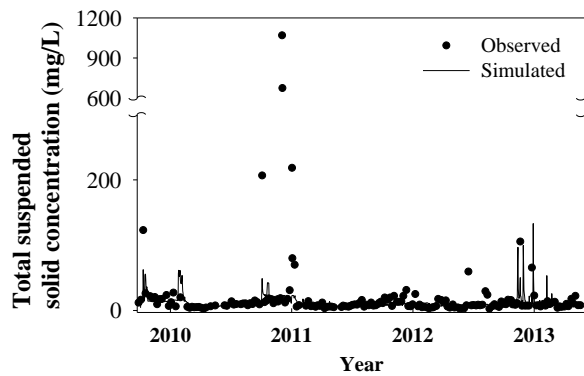
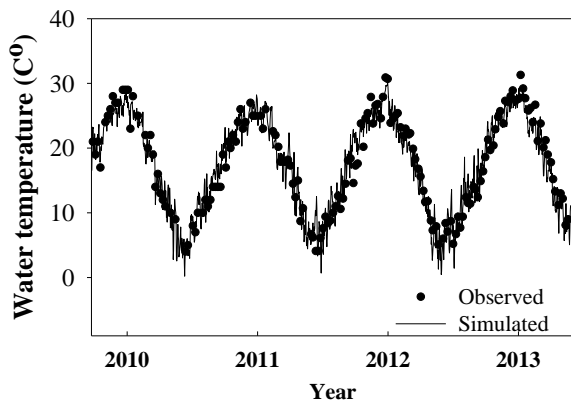


(e)

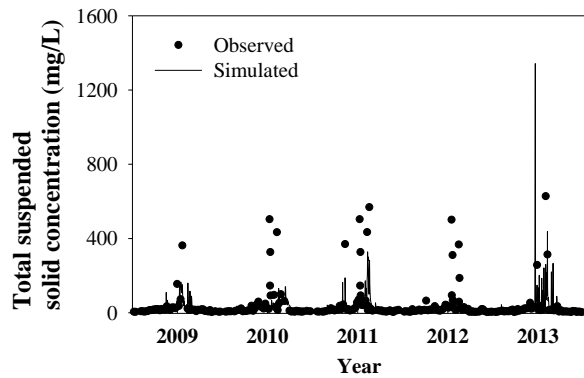
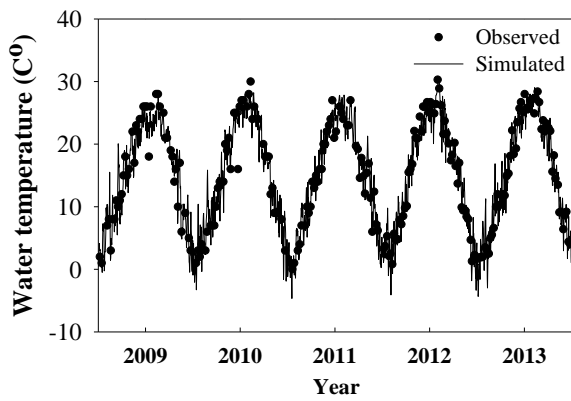
Fig. S2: Meteorological data during the simulation period in 2011 and 2012. (a) atmospheric pressure (mb), (b) air temperature ($^{\circ}\text{C}$), (c) humidity ($\%/100$), (d) solar radiation (J/s/m^2), and (e) cloud cover (-).



(a) Main stream



(b) Gap stream



(c) Miho stream

Fig. S3. Comparison of measured and simulated water temperatures and suspended sediment concentrations at each stream.

Table S3: Range of model parameters for OAT method with reference (calibrated) value (red zone) and for Morris screening method (blue zone).

Input parameter	Unit	Morris screening method				
		Min.	-----			Max.
		OAT method				
		-50%	Reference (Calibrated) value	+50%		
Settling velocity (w_s)	m/s	9.0×10^{-6}	1.1×10^{-4}	2.2×10^{-4}	3.3×10^{-4}	2.0×10^{-3}
Critical deposition stress (τ_{cd})	N/m ²	2.0×10^{-2}	1.0×10^{-1}	2.0×10^{-1}	3.0×10^{-1}	1.1×10^0
Critical erosion stress (τ_{ce})	N/m ²	1.2×10^{-1}	2.0×10^{-1}	4.0×10^{-1}	6.0×10^{-1}	9.3×10^{-1}
Cd partitioning coefficient between suspended sediment and water ($K_{d,SS}$)	L/mg	5.0×10^{-3}	3.95×10^{-2}	7.9×10^{-2}	1.19×10^{-1}	1.3×10^0
Cd partitioning coefficient between sediment bed and water ($K_{d,bed}$)	L/mg	3.2×10^{-6}	1.0×10^{-3}	2.0×10^{-3}	3.0×10^{-3}	4.2×10^0

* The main reason for selecting 50% variation for the OAT method was to effectively cover the parameter ranges as reported in the literature. However, the range of critical erosion stress in the literature was admittedly narrower and therefore the coverage was not similar across all the parameter inputs.

Table S4: Formulations for quantifying the discrepancy between model outputs and measured concentrations.

Index	Equation
<i>Absolute Mean Error (AME)</i>	$AME = \frac{1}{N} \sum_{n=1}^N O^n - P^n $
<i>Root Mean Square Error (RMSE)</i>	$RMSE = \sqrt{\frac{1}{N} \sum_{n=1}^N (O^n - P^n)^2}$
<i>Relative Error (RE)</i>	$RE = \frac{AME}{\text{Observed Mean}} \times 100 = \frac{\frac{1}{N} \sum_{n=1}^N O^n - P^n }{\bar{O}} \times 100$
<i>Relative Root Mean Square Error (RRMSE)</i>	$RRMSE = \frac{RMSE}{\text{Observed Change}} \times 100 = \frac{\sqrt{\frac{1}{N} \sum_{n=1}^N (O^n - P^n)^2}}{O_{max} - O_{min}} \times 100$

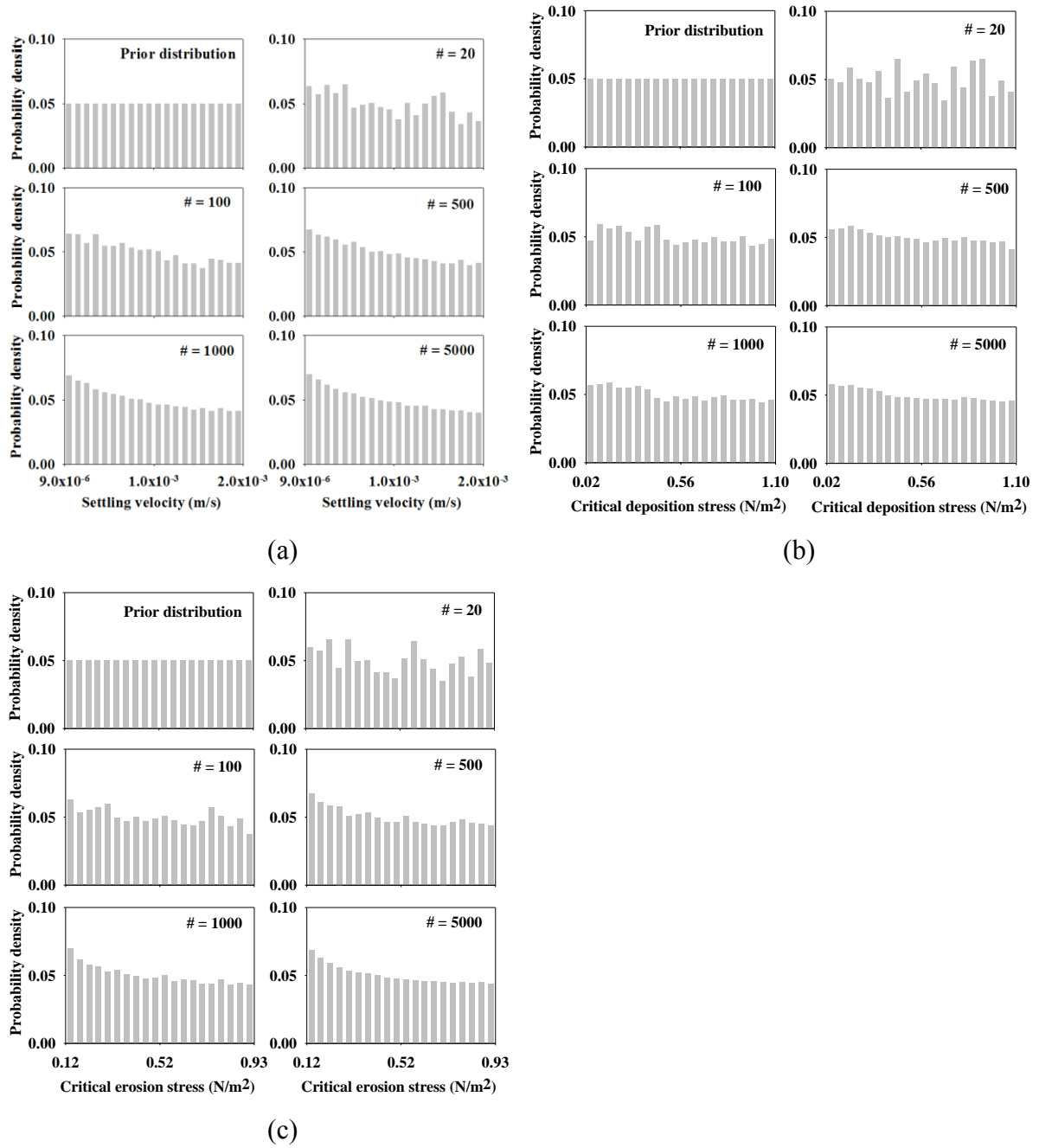


Fig. S4: Prior and posterior parameter distributions when data collected only in Period 1 were used for updating the model: (a) settling velocity, (b) critical deposition stress, and (c) critical erosion stress.

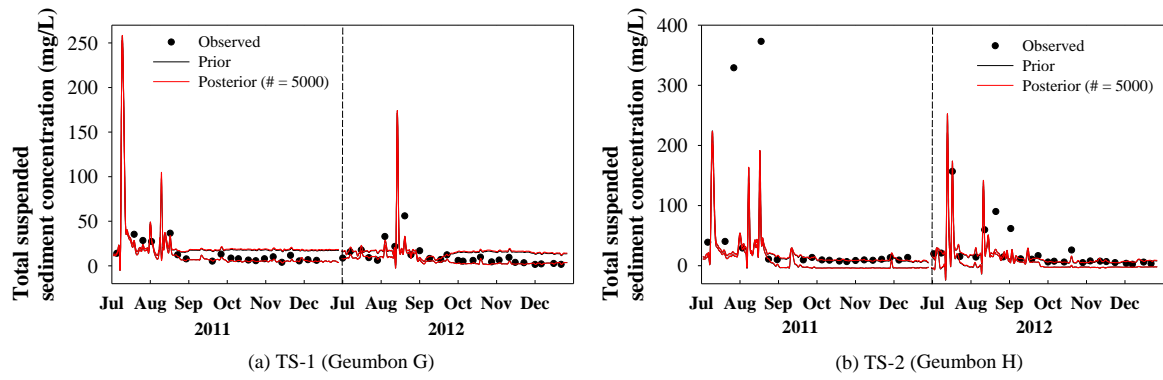


Fig. S5: Prior and posterior predictive distributions of the total suspended sediment concentrations when data collected only in Period 1 were used for updating the model.

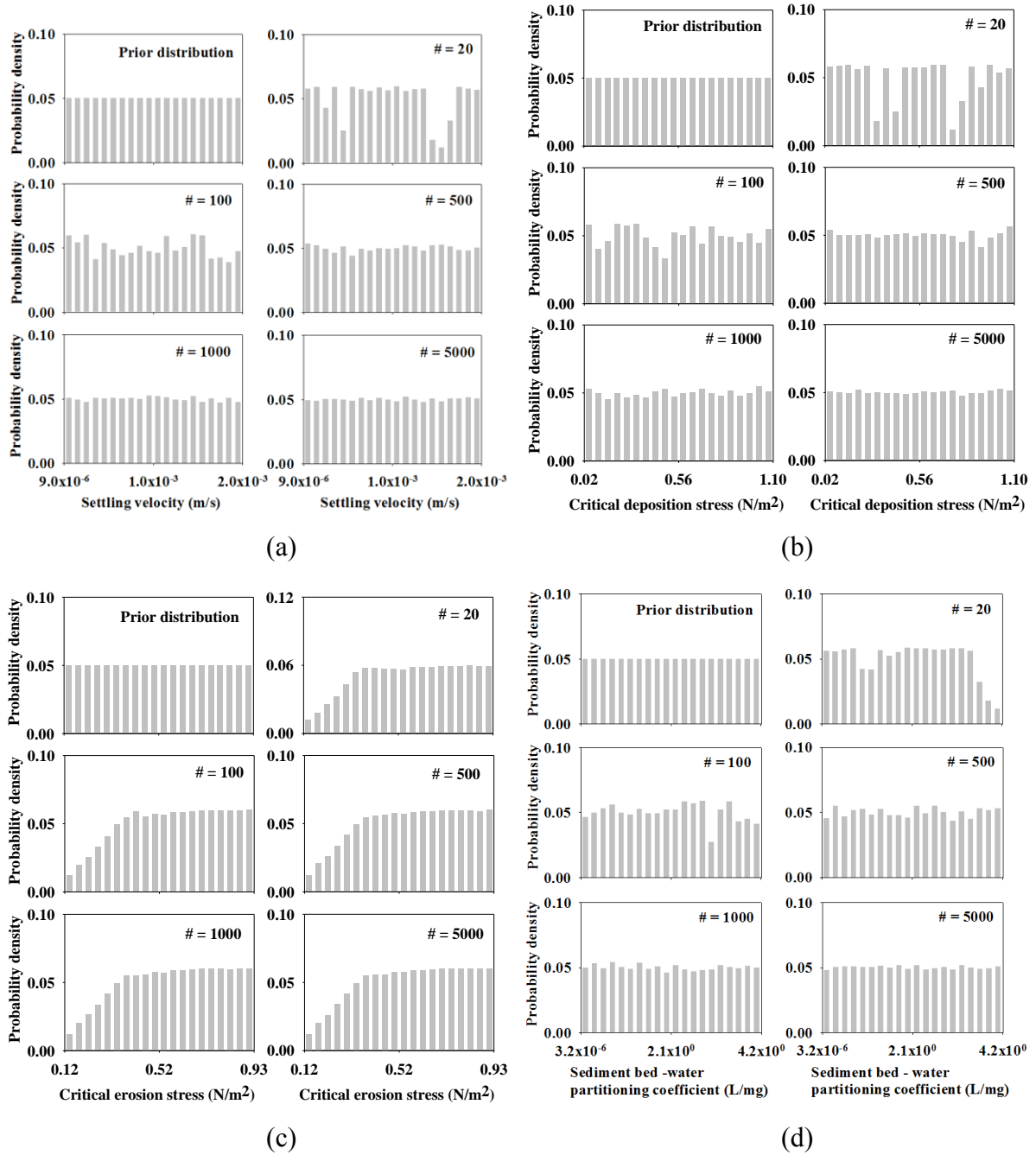


Fig. S6: Prior and posterior parameter distributions when total metal (*Cd*) concentration data were used for updating the model: (a) settling velocity, (b) critical deposition stress, (c) critical erosion stress, and (d) sediment bed-water *Cd* partitioning coefficient.

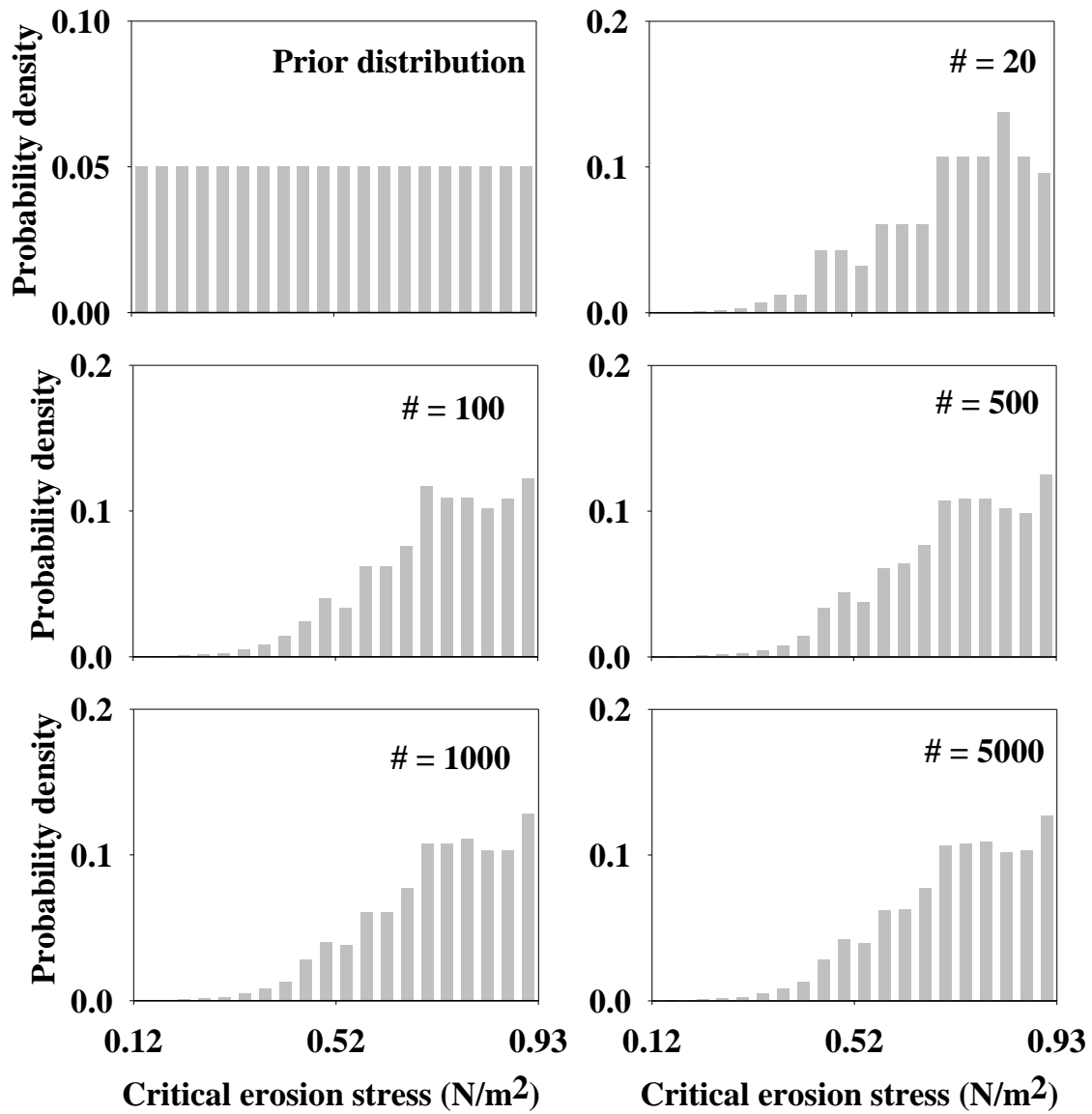
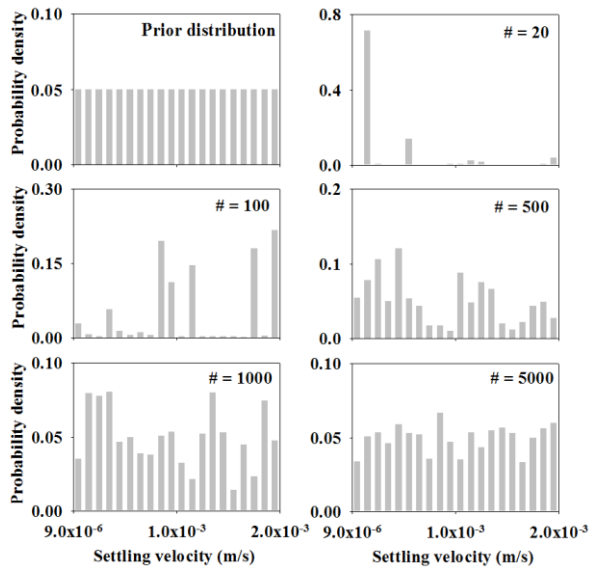
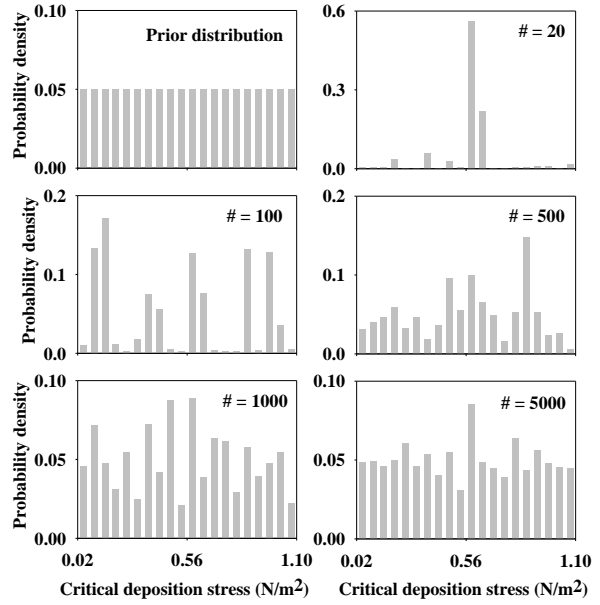


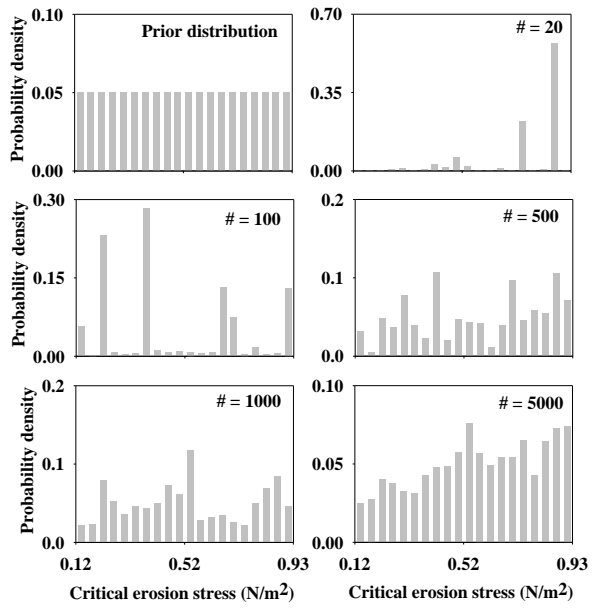
Fig. S7. Prior and posterior distributions of the critical erosion stress using total metal concentration data collected only in 2011 for updating the model.



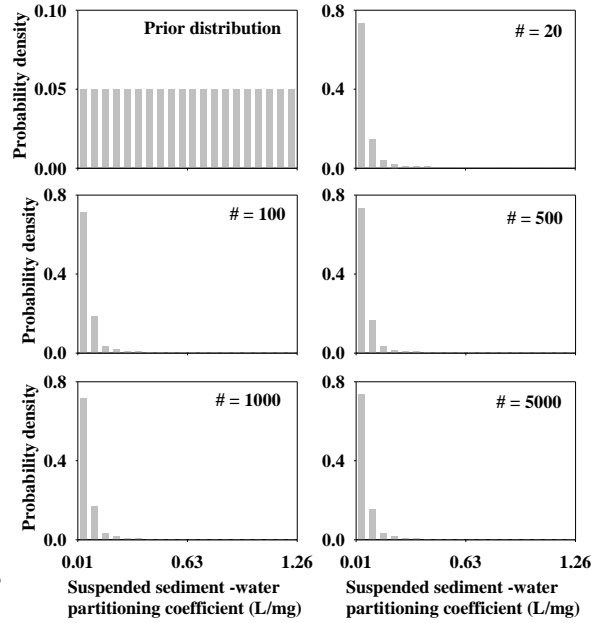
(a)



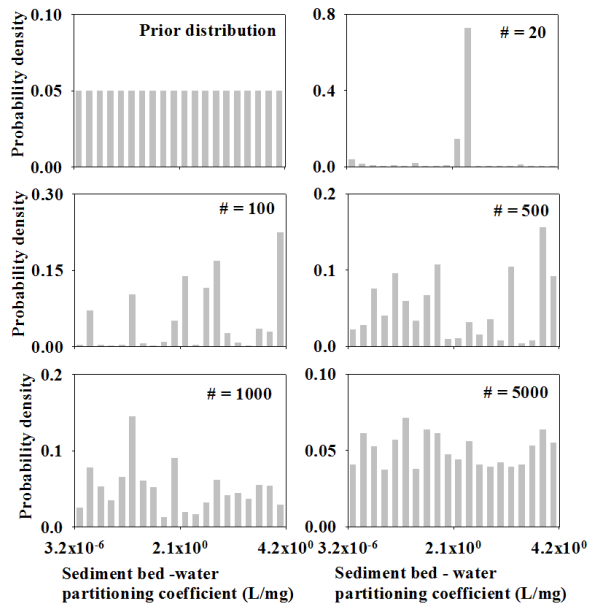
(b)



(c)



(d)



(e)

Fig. S8: Prior and posterior parameter distributions when the entire dissolved metal (*Cd*) concentration data were used for updating the model: (a) settling velocity, (b) critical deposition stress, (c) critical erosion stress, (d) suspended sediment-water *Cd* partitioning coefficient, and (e) sediment bed-water *Cd* partitioning coefficient.